Descriptive anatomy of the largest known specimen of *Protoichthyosaurus prostaxalis* (Reptilia: Ichthyosauria) including computed tomography and digital reconstruction of a three-dimensional skull (#29904)

First submission

Editor guidance

Please submit by **27 Aug 2018** for the benefit of the authors (and your $200 publishing discount).

Structure and Criteria
Please read the 'Structure and Criteria' page for general guidance.

Author notes
Have you read the author notes on the guidance page?

Raw data check
Review the raw data. Download from the location described by the author.

Image check
Check that figures and images have not been inappropriately manipulated.

Privacy reminder: If uploading an annotated PDF, remove identifiable information to remain anonymous.

Files
Download and review all files from the materials page.

9 Figure file(s)
1 Table file(s)
3 Other file(s)

Structure and Criteria

Structure your review

The review form is divided into 5 sections. Please consider these when composing your review:

1. **BASIC REPORTING**
2. **EXPERIMENTAL DESIGN**
3. **VALIDITY OF THE FINDINGS**
4. General comments
5. Confidential notes to the editor

You can also annotate this PDF and upload it as part of your review

When ready submit online.

Editorial Criteria

Use these criteria points to structure your review. The full detailed editorial criteria is on your guidance page.

BASIC REPORTING

- Clear, unambiguous, professional English language used throughout.
- Intro & background to show context. Literature well referenced & relevant.
- Structure conforms to PeerJ standards, discipline norm, or improved for clarity.
- Figures are relevant, high quality, well labelled & described.
- Raw data supplied (see PeerJ policy).

EXPERIMENTAL DESIGN

- Original primary research within Scope of the journal.
- Research question well defined, relevant & meaningful. It is stated how the research fills an identified knowledge gap.
- Rigorous investigation performed to a high technical & ethical standard.
- Methods described with sufficient detail & information to replicate.

VALIDITY OF THE FINDINGS

- Impact and novelty not assessed. Negative/inconclusive results accepted. *Meaningful* replication encouraged where rationale & benefit to literature is clearly stated.
- Data is robust, statistically sound, & controlled.
- Speculation is welcome, but should be identified as such.
- Conclusions are well stated, linked to original research question & limited to supporting results.

Standout reviewing tips

The best reviewers use these techniques

Tip	*Example*
Support criticisms with evidence from the text or from other sources	*Smith et al (J of Methodology, 2005, V3, pp 123) have shown that the analysis you use in Lines 241-250 is not the most appropriate for this situation. Please explain why you used this method.*
Give specific suggestions on how to improve the manuscript	*Your introduction needs more detail. I suggest that you improve the description at lines 57- 86 to provide more justification for your study (specifically, you should expand upon the knowledge gap being filled).*
Comment on language and grammar issues	*The English language should be improved to ensure that an international audience can clearly understand your text. Some examples where the language could be improved include lines 23, 77, 121, 128 – the current phrasing makes comprehension difficult.*
Organize by importance of the issues, and number your points	*1. Your most important issue* *2. The next most important item* *3. …* *4. The least important points*
Please provide constructive criticism, and avoid personal opinions	*I thank you for providing the raw data, however your supplemental files need more descriptive metadata identifiers to be useful to future readers. Although your results are compelling, the data analysis should be improved in the following ways: AA, BB, CC*
Comment on strengths (as well as weaknesses) of the manuscript	*I commend the authors for their extensive data set, compiled over many years of detailed fieldwork. In addition, the manuscript is clearly written in professional, unambiguous language. If there is a weakness, it is in the statistical analysis (as I have noted above) which should be improved upon before Acceptance.*

Descriptive anatomy of the largest known specimen of *Protoichthyosaurus prostaxalis* (Reptilia: Ichthyosauria) including computed tomography and digital reconstruction of a three-dimensional skull

Dean R. Lomax Corresp., [1] , **Laura B. Porro** [2] , **Nigel R. Larkin** [3]

[1] School of Earth and Environmental Sciences, University of Manchester, Manchester, United Kingdom
[2] School of Earth Sciences, University of Bristol, Bristol, United Kingdom
[3] Cambridge University Museum of Zoology, Cambridge, United Kingdom

Corresponding Author: Dean R. Lomax
Email address: dean.lomax@manchester.ac.uk

Ichthyosaur fossils are abundant in Lower Jurassic sediments with nine genera found in the UK. A large undescribed partial ichthyosaur skeleton from the Lower Jurassic (lower Sinemurian) of Warwickshire, England was conserved and the skull rearticulated to form the centerpiece of a new permanent gallery at the Thinktank, Birmingham Science Museum in 2015. In this paper, we describe the skull and postcranial skeleton of this specimen for the first time. The unusual three-dimensional preservation of the specimen permitted computed tomography scanning of individual braincase elements as well as the entire reassembled skull. This represents one of the first times that medical imaging and three-dimensional reconstruction methods have been successfully applied to the skull of a large marine reptile. Data from these scans provide new anatomical information, such as the presence of long, branching vascular canals within the premaxilla and dentary, as well as an undescribed dorsal wing of the pterygoid hidden within matrix. Scanning also revealed areas of the skull that had been modelled in wood, clay and other materials after the specimen's initial discovery, highlighting the utility of applying advanced imaging techniques to historical specimens. Additionally, the CT data served as the basis for a new three-dimensional reconstruction of the skull of this specimen, in which minor damage was repaired and the preserved bones properly rearticulated. Museum records show the specimen was originally identified as an example of *Ichthyosaurus communis* but based on our examination we identify this specimen as *Protoichthyosaurus prostaxalis*. The specimen features a skull nearly twice as long as any previously described specimen of *P. prostaxalis,* representing an individual with an estimated total body length between 3.2 and 4 meters.

Descriptive anatomy of the largest known specimen of *Protoichthyosaurus prostaxalis* (Reptilia: Ichthyosauria) including computed tomography and digital reconstruction of a three-dimensional skull

Dean R. Lomax[1], Laura B. Porro[2], Nigel R. Larkin[3]

[1] School of Earth and Environmental Sciences, The University of Manchester, Oxford Rd, Manchester, M13 9PL, United Kingdom

[2] School of Earth Sciences, University of Bristol, Life Sciences Building, 24 Tyndall Avenue, Bristol, BS8 1TQ, United Kingdom

[3] Cambridge University Museum of Zoology, Downing St, Cambridge, CB2 3EJ, United Kingdom

Corresponding Author: Dean R. Lomax, dean.lomax@manchester.ac.uk

Abstract

Ichthyosaur fossils are abundant in Lower Jurassic sediments with nine genera found in the UK. In this paper, we describe the partial skeleton of a large ichthyosaur from the Lower Jurassic (lower Sinemurian) of Warwickshire, England, which was conserved and rearticulated to form the centerpiece of a new permanent gallery at the Thinktank, Birmingham Science Museum in 2015. The unusual three-dimensional preservation of the specimen permitted computed tomography scanning of individual braincase elements as well as the entire reassembled skull. This represents one of the first times that medical imaging and three-dimensional reconstruction methods have been applied to the skull of a large marine reptile. Data from these scans provide

new anatomical information, such as the presence of branching vascular canals within the premaxilla and dentary, and an undescribed dorsal wing of the pterygoid hidden within matrix. Scanning also revealed areas of the skull that had been modelled in wood, clay and other materials after the specimen's initial discovery, highlighting the utility of applying advanced imaging techniques to historical specimens. Additionally, the CT data served as the basis for a new three-dimensional reconstruction of the skull, in which minor damage was repaired and the preserved bones digitally rearticulated. Museum records show the specimen was originally identified as an example of *Ichthyosaurus communis* but we identify this specimen as *Protoichthyosaurus prostaxalis*. The specimen features a skull nearly twice as long as any previously described specimen of *P. prostaxalis,* representing an individual with an estimated total body length between 3.2 and 4 meters.

Key words Ichthyosauria, Ichthyosauridae, visualization, CT-scanning

Introduction

Ichthyosaurs were a highly successful group of predatory marine reptiles that appeared in the late Early Triassic and went extinct in the early Late Cretaceous. Some of the earliest forms were 'lizard-like' in appearance, although later forms evolved fish-shaped bodies (Motani, 2009). Species ranged in size from small-bodied forms less than 1 m long to giants over 20 m in length (Motani, 2005; Nicholls & Manabe, 2004; Lomax et al., 2018). Numerous Lower Jurassic ichthyosaurs have been found in the UK, the majority being from the Lyme Regis-Charmouth area in west Dorset (Milner & Walsh, 2010), the village of Street and surrounding areas in Somerset (Delair, 1969), sites around the coastal town of Whitby, Yorkshire (Benton & Taylor,

1984) and Barrow-upon-Soar, Leicestershire (Martin et al., 1986). Notable specimens have also been recorded from Ilminster, Somerset (Williams et al., 2015), Nottinghamshire (Lomax & Gibson, 2015) and Warwickshire (Smith & Radley, 2007), with various isolated occurrences at other sites across the UK (Benton & Spencer, 1995).

A partial ichthyosaur skeleton (BMT 1955.G35.1 – Birmingham Museums Trust) was discovered in 1955 in Warwickshire. The specimen comprises a largely complete skull, portions of the pectoral girdle, pelvis, fore- and hindfins, and numerous vertebrae and ribs. Bones of the basicranium and palate, which are rarely observed in association with Lower Jurassic ichthyosaur skulls, were found (Marek et al., 2015). The skull bones were reassembled three-dimensionally on a wood and metal frame held together with alvar, jute and kaolin dough, with missing parts carved from wood; however, some aspects were not accurately reconstructed. Museum records indicate that BMT 1955.G35.1, which has never been formally described, was originally identified as an example of *Ichthyosaurus communis*.

In 2015, as part of the development of the new Marine Worlds Gallery at the Thinktank, Birmingham Science Museum, the skull was dismantled, conserved and reassembled to be more anatomically accurate. The skull and postcranial skeleton of BMT 1955.G35.1 were publicly displayed for the first time, forming the centerpiece of this permanent gallery. The skull of BMT 1955.G35.1 is preserved in 3D; this contrasts with the majority of Lower Jurassic specimens, which are flattened, enabling a more detailed description than is typical. The large size of many marine reptile skulls has precluded attempts to visualize specimens using medical imaging (but see McGowan, 1989). Given the exceptional 3D preservation, the fact it is relatively free of matrix, and access to facilities capable of imaging large specimens, we took the opportunity to scan individual cranial elements as well as the entire skull of BMT 1955.G35.1 using computed

tomography (CT) before and after reassembly. Computed tomography and 3D digital reconstruction are increasingly being applied to the skulls of fossil vertebrates, including early tetrapods (Porro et al., 2015*a,b*), dinosaurs (Rayfield et al., 2001; Lautenschlager et al., 2014, 2016; Porro et al., 2015c; Button et al., 2016) and extinct synapsids (Wroe, 2007; Jasinoski et al., 2009; Sharp, 2014; Cox et al., 2015; Lautenschlager et al., 2017). In contrast, these methods have been applied only to isolated regions of fossil marine reptile skulls (Kear, 2005; Fernández et al., 2011; Sato et al., 2011; Neenan and Scheyer, 2012; Herrera et al., 2013), with the exception of one pliosaur (Foffa et al., 2014), one small ichthyosaur (Marek et al., 2015), for which entire skulls were CT scanned, and the skeleton of a juvenile plesiosaur (Larkin et al., 2010).

In this paper, we use CT scanning of a large ichthyosaur skull along with careful examination of the original specimen to formally describe BMT 1955.G35.1. Based on this description we reassign the specimen to *Protoichthyosaurus prostaxalis* Appleby 1979, a genus recently shown to be distinct from *Ichthyosaurus* based on multiple characters (Lomax, Massare & Mistry, 2017; Lomax & Massare, 2018). Furthermore, the studied specimen has a skull and estimated total body length greater than any known specimen of *Protoichthyosaurus* or *Ichthyosaurus*.

Geological setting

BMT 1955.G35.1 was collected in situ from Fell Mill Farm, between Shipston-on-Stour and Honington, Warwickshire, England, grid reference NGR SP 277 415. The initial discovery was made by Mr Michael Bryan in May, 1955. A complete excavation, under the supervision of assistant keeper of natural history at the City of Birmingham Museum, Mr Vincent Smith, subsequently took place. The specimen was found approximately 4 feet below the ground surface

in a hard, blue-grey clay, lying directly on top of a brown grit layer containing numerous *Gryphaea* bivalves. Due to the fragmentary nature of the bones, they were removed embedded in clay.

Precise stratigraphic data associated with the discovery are not available but the remains were recorded as being from Liassic sediments, which conforms to the Early Jurassic age of the region's geology (Edmonds et al., 1965; Radley, 2003; Smith & Radley, 2007). In addition to the ichthyosaur skeleton, other fossils were collected alongside the specimen, including *Gryphaea* bivalves, a plesiosaur vertebra, and an isolated shark tooth identified as *Hybodus* cf. ~~*H.*~~ *cloacinus* Quenstedt 1895, which are also Early Jurassic in age, although this shark species ranges from the Rhaetic through Lower Lias (N. R. Larkin, pers. comm. D. Ward, 2015). Additionally, we found an ammonite fragment stored with the specimen, which is an example of *Euagassiceras sauzeanum* (d'Orbigny), a species indicative of the Semicostatum Ammonite Zone, lower Sinemurian, Lower Jurassic (DRL pers. comm. M. Howarth, 2017). As there was no record stating whether this ammonite fragment was physically collected with BMT 1955.G35.1, NRL was given permission by the current owners of Fell Mill Farm to collect other fossils along with matrix from the original site at a depth of 2 m below the surface. This resulted in the collection of numerous ammonites identified as *Arnioceras semicostatum* (Young & Bird), which is also indicative of the lower Sinemurian, Semicostatum Ammonite Zone (DRL pers. comm. M. Howarth, 2017). Thus, associated ammonites have provided the stratigraphic position of BMT 1955.G35.1.

Material and methods

BMT 1955.G35.1 is currently housed in the Thinktank Science Museum (TSM). It was originally accessioned into the collections of Birmingham Museum and Art Gallery (BMAG) and loaned to TSM. However, BMAG and TSM have since become part of the Birmingham Museums Trust (BMT). The postcranial skeleton, long considered 'missing', was rediscovered in the collections of the Lapworth Museum of Geology (BU) and reunited with the skull as part of a funded project at the TSM. As BMT 1955.G35.1 was largely undeformed, the individual skull bones were assembled in 3D; however, several errors were made in this original reconstruction (Fig. 1A). As part of the funded project, the skull was disassembled and the individual bones cleaned, conserved, and remounted (Fig. 1B-C). Many of the preserved skull bones were disarticulated when discovered and several cranial bones are not represented. The teeth have been reset and are not in their original positions. Portions of some elements are poorly preserved and/or taphonomically distorted, which somewhat restricts our description; for example, the dentaries cannot be articulated at the symphysis or mounted in their correct anatomical position. The newly reassembled skull of BMT 1955.G35.1 is based on all the preserved elements robust enough to safely include, and we limit our description of sutural contacts to those between elements preserved in original articulation. Specific details of the reconstruction and conservation of the studied specimen will be dealt with in a separate paper.

Prior to remounting, several individual bones of the left side of the skull were scanned using microcomputed tomography (μCT) in March 2015 at the Cambridge Biotomography Centre (Zoology Department, University of Cambridge) on an X-Tek H 225 μCT scanner (Nikon Metrology, Tring, UK) at 135kV and 227 μA. Elements scanned individually include: the left articular, opisthotic, stapes, quadrate and pterygoid; the median supraoccipital and basisphenoid; and both parietals. Voltage, current and resolution (0.1 mm/voxel) were identical for all scans.

Scan data were visualized in the software Avizo 8.0 (Thermo Fisher Scientific, Waltham, Massachusetts, USA) and the left-side elements mirrored across the sagittal midline. All 3D surfaces were exported as stereolithography (STL) files and 3D printed at life-size in gypsum on a 3DS x60 3D Printer; pieces were subsequently dipped in cyanoacrylate for strength (NRL pers. comm. S. Dey, 2016).

After remounting, the skull of BMT 1955.G35.1, including the 3D printouts previously described, was scanned in May 2015 at the Royal Veterinary College on a Lightspeed Pro 16 CT scanner (GE Medical Systems LTd., Pollards Wood, UK) at 120 kV and 200 µA. Due to the size of the specimen, it was scanned in two parts – the front of the skull was scanned at 0.56x0.56x1.25 mm/voxel and the rear of the skull was scanned at 0.73x0.73x1.25 mm/voxel. Both scans produced a total of 2168 DICOM slices. Density thresholding was used to separate higher-density fossil bone from lower-density matrix as well as areas of the skull historically modelled in wood, clay and jute, and portions newly modelled in gypsum. Scans were segmented to isolate individual bones and teeth, and to trace internal features. The two halves of the skull were overlain and merged using skeletal landmarks visible in both datasets (Figs. 2-4). Three-dimensional surfaces were exported as wavefront (OBJ) files to create an interactive 3D PDF using Tetra4D Reviewer and Converter (Tech Soft 3D; Oregon, USA) and Adobe Acrobat Pro X (Adobe Systems, California, USA). This reconstruction is provided as supporting information (Appendix S1) and are the basis for the following description.

Surface models of individual bones were manipulated in 3D space using the Transform Editor within Avizo, allowing digital 3D reconstruction of the skull of BMT 1955.G35.1 following similar methods applied to fossil tetrapods (Porro et al. 2015*a,b*) and dinosaurs (Lautenschlager, 2016). Most of the bones in the digital reconstruction are from the left side of

BMT 1955.G35.1 as this side is generally better preserved. Minor damage was manually repaired in the Segmentation Editor within Avizo using interpolation, including: minor breaks and missing alveolar margins in the left premaxilla, maxilla, dentary and splenial; minor breaks in the left nasal, lacrimal, jugal, quadrate, pterygoid, and parietal; the missing right margin of the supraoccipital; and gaps within the anterior half of the left surangular. Portions of bones preserved on the right but absent on the left – including the posterior tip of the right jugal and anterior tip of the right splenial – were duplicated, reflected across the sagittal midline, and merged with left side elements using anatomical landmarks. We did not attempt to reconstruct missing bones or preserved elements that could not be scanned due to their delicate nature (see Results). The disarticulated bones were then fitted together at sutural contacts; we also referred to known relationships between skull bones from other ichthyosaur skulls (Andrews, 1910; McGowan, 1973; Kirton, 1983; McGowan & Motani, 2003; Marek et al., 2015). Lastly, left side elements were duplicated and reflected to form the right side of the skull. Transformation matrices for all bones from the original data set to the final 3D reconstruction are available as supporting information (Appendix S2); a 3D PDF of the reconstructed skull is also available as supporting information (Appendix S3).

Institutional abbreviations

BMT, Birmingham Museums Trust (encompasses BMAG, Birmingham Museum and Art Gallery and TSM, Thinktank, Birmingham Science Museum), UK; BRLSI, Bath Royal Literary and Scientific Institution, Bath, UK; ~~BU,~~ Lapworth Museum of Geology, University of Birmingham, UK; LEICT, Leicester Arts and Museums Service, New Walk Museum and Art Gallery, Leicester, UK; NHMUK, Natural History Museum, London, UK; SOMAG (formerly

AGC), Alfred Gillett Collection, cared for by the Alfred Gillett Trust (C & J Clark Ltd), Street, Somerset, UK; ~~UNM~~, University of Nottingham Museum, UK.

Systematic Palaeontology

Ichthyosauria de Blainville, 1835

Parvipelvia Motani, 1999

Ichthyosauridae Bonaparte, 1841

Protoichthyosaurus Appleby, 1979

Protoichthyosaurus prostaxalis Appleby, 1979

Type species. *P. prostaxalis* Appleby 1979. The type series of specimens are from historic collections. However, the holotype is most likely from the area around Street, Somerset and is most likely from the lowermost Jurassic (lower Hettangian) 'Pre-Planorbis Beds' (i.e., Tilmanni Ammonite Zone) of the Blue Lias Formation, although it could be latest Triassic (Rhaetian). See Lomax et al., (2017) for more details.

Holotype. BRLSI M3553, a partial skull, pectoral girdle, and both forefins, preserved in ventral view.

Paratypes. BRLSI M3555, a skull and partial skeleton, preserved in right lateral view; BRLSI M3563, a composite partial skeleton; LEICT G454.1951/164, a partial forefin, presently missing, which might be a hindfin of a different genus (see Lomax, Massare & Mistry, 2017 for more details).

Referred specimen. BMT 1955.G35.1, an almost complete, three-dimensional skull and partial postcranial skeleton.

Emended diagnosis. As in Lomax et al., (2017), but with the following change: total length greater than 3.2 m but probably less than 4 m.

Occurrence. Fell Mill Farm, between Shipston-on-Stour and Honington, Warwickshire, England, grid reference NGR SP 277 415. The specimen was collected from blue-grey Liassic clay, and specifically from the Semicostatum Ammonite Zone, lower Sinemurian, Lower Jurassic.

Results

Anatomical description of the skull roof

Measurements of the skull are presented in Table 1. In lateral view, the upper jaw is shaped like a right-angle triangle, the ventral margin being nearly straight and dorsal surface of the snout being gently sloped (Fig. 1). In dorsal and ventral views, the anterior snout (formed by the premaxillae) is shaped like a finely pointed triangle (Fig. 2); the posterior cranium is mediolaterally expanded. Preserved bones of the skull roof (Figs 1-2, 5) include most of the premaxillae, both maxillae, partial nasals, partial left lacrimal, partial prefrontals and postfrontals, complete left and partial right jugals, nearly complete parietals, and partial supratemporals. Some of these elements (e.g. portions of nasal and postfrontals) were too fragmentary and/or poorly preserved to attach to the skull and are not part of the 3D model. The left postorbital was originally present (Fig. 1A), but we were unable to locate the element. The

quadratojugals and squamosals are not preserved in BMT 1955.G35.1. The frontals are also missing with the exception of a small fragment attached to the left nasal. Unless otherwise stated, the morphology concurs with other specimens of the species (Lomax, Massare & Mistry, 2017; Lomax & Massare, 2018).

Premaxilla. The premaxilla makes up two-thirds of the cranium and most of the snout. The majority of both premaxillae are preserved, although portions of the posterior ends are missing including the margin of the external naris (Figs 1-2). The left premaxilla is more complete than the right element. In lateral view, the anterior premaxilla is dorsoventrally low but becomes progressively taller posteriorly. A longitudinal groove exposing a series of foramina (see below) along the lateral surface represents the fossa praemaxillaris (Figs 1B-C, 2). The right premaxilla preserves a long, tapering subnarial process that articulates with the maxilla and extends to the middle of the maxilla (Figs 1B, 2A); the supranarial process is not preserved on either side. Laterally, the contact between the premaxilla and maxilla is clear and consists of an extensive scarf joint in which the ventral margin of the premaxilla laterally and dorsally overlaps the anterior process of the maxilla (Figs 1-2). The contact between the premaxilla and maxilla on the palate is difficult to discern, although it appears that a maxillary shelf extends medially and replaces the premaxillary shelf at the level of the 18th preserved tooth on the right side. (The teeth, were reset during conservation and their positions in the jaw are not original. However, their reconstructed positions act as landmarks for our description.) Except at the anterior tip of the snout, the premaxillae do not meet at the ventral midline.

In dorsal view, the premaxillae would have contacted each other at a butt joint for much of their length, although they are largely separated due to deformation (Fig. 2E). Posteriorly, the

nasals inserted between the premaxillae. The dorsal margin of the left premaxilla laterally and dorsally overlaps the nasal from approximately the level of the 13th premaxillary tooth to its broken posterior end. In dorsal view, a small, narrow portion of the anterior process of the nasal is exposed; the rest is overlapped by the premaxilla.

Anteriorly, the premaxilla is a laterally bowed sheet of bone in transverse cross-section; at the level of the seventh preserved tooth, it develops a medial shelf that roofs the alveolar groove. From this point until its articulation with the maxilla, the premaxilla consists of a ventral lamina that laterally overlaps the teeth, the medial shelf, and a dorsal lamina, which is deeply grooved along its margin on the right side, presumably to receive the nasal. CT scans reveal that each premaxilla encloses a branching, longitudinal canal dorsal to the tooth row (Fig. 2G-J). This canal extends from the posterior end of the premaxillary tooth row to the third premaxillary tooth. Anteriorly, a series of short canals branch anterolaterally from the main conduit and open onto the fossa praemaxillaris, either immediately above the alveolar margin or on the dorsolateral aspect of the bone. The right premaxilla preserves five ventral and four dorsal foramina; the left premaxilla preserves four ventral and one dorsal foramina. The posterior half of each premaxilla contains two longer canals branching posteriorly from the main conduit, each of which opens onto posteriorly elongated grooves parallel to the alveolar margin of the premaxilla. The left premaxilla preserves two additional longitudinal grooves on the posterior half of its dorsolateral surface; however, these do not connect to the main canal within the premaxilla.

Maxilla. Both maxillae are preserved, although the posterior portion of the left maxilla is missing and both are damaged. In lateral view, the maxilla is a triangular bone with slender anterior and posterior processes and is dorsoventrally tallest in its center (Figs 1-2). The anterior process is

longer and more delicate than the posterior process, which extends just under the orbit. Although the external naris is not preserved, it is clear the maxilla extended well beyond the anterior end of the external naris.

The alveolar groove of the maxilla is continuous with that of the premaxilla. In transverse section, the anterior maxilla has a ventral lamina that extends lateral to the tooth row, a ventrally curving medial shelf (forming the dorsal and medial walls of the alveolar groove) and a short dorsal lamina that contacts the medial surface of the premaxilla in a scarf joint. The dorsal lamina of the maxilla, which underlaps the premaxilla, is exposed slightly anterior to the middle of the left maxilla due to the damaged premaxilla. Posterior to the main body, the maxilla is triangular in transverse section with a ridge on its dorsomedial surface that appears to articulate with the short anterior process of the lacrimal, which is poorly preserved. An articulation surface on the dorsolateral surface of the posterior process of the maxilla meets the jugal in a scarf joint, separating the posterior process of the maxilla from the lacrimal.

Nasal. The anterolateral portion of the left nasal is preserved attached to the premaxilla (Figs 1-2). It is best seen in ventral and posterior views, which reveals it is dorsoventrally thickened medially but becomes dorsoventrally thin laterally. The bone is laterally bowed in transverse section. The ventral margin of the nasal is laterally overlapped by the dorsal lamina of the premaxilla; the morphology of the right premaxilla suggests this may have originally been a tongue-and-groove contact. Near the posterior end of the element is a small fragment featuring a grooved medial margin; it is unclear if this is a portion of the nasal or a fragment of the frontal. CT scans reveal a few short canals penetrating the nasal from its lateral surface.

Other fragments of the nasal were found with the specimen but not mounted on the skull due to their fragile nature. Much of the right nasal is preserved although the posterior end is missing and it is impossible to determine the presence of an internasal foramen. It is a long and delicate element that is wide posteriorly, and tapers to a point anteriorly. On the left lateral surface is a long groove that runs almost the entire length of the nasal. The slightly flared right lateral wing is damaged. Two foramina are present posteriorly, positioned next to a portion of what may be the prefrontal.

Lacrimal. The left lacrimal is poorly preserved. It appears to be triradiate with a short, but damaged anterior process and a longer posteroventral process. The dorsal process is tall and formed the posterior margin of the external naris. It was clearly excluded from the orbital margin by the anterior process of the prefrontal (Figs 1B, 2B,D). The lateral surface of the dorsal process preserves external sculpting and several canals that penetrate the bone but cannot be traced. The short, tapering anterior process fits onto a shelf on the dorsomedial aspect of the maxilla. The posteroventral process, which is longer and mediolaterally wider than the anterior process, is complete and contributes to the anteroventral margin of the orbit. It meets the dorsal margin of the jugal in a curving contact. The lateral surface of the posteroventral process bears the remnant of a ridge from its posterior tip to the base of the dorsal process.

Prefrontal. Only a small portion of the anterior process of the left prefrontal is present, although original photographs of the mounted skull show that the element was once complete (Figs 1B, 2B). The anterior process of the prefrontal medially and dorsally laps the lacrimal along a broad

contact, where it is dorsoventrally tall and excludes the dorsal process of the lacrimal from the orbit.

Postfrontal. The anterior portions of both postfrontals are preserved but were not added to the mount. The right postfrontal is the more complete of the two. In dorsal view, the anterior end is mediolaterally broad and dorsoventrally thin. The postfrontal narrows posteriorly, where it is damaged. The medial surface exhibits a prominent ridge.

Jugal. The jugal is a long, slender bone forming the ventral margin of the orbit; the left is better preserved than the right (Figs 1-2). Anteriorly it is oval-shaped in transverse section and tapers to a point, contacting the posteroventral margin of the lacrimal and dorsolateral aspect of the posterior process of the maxilla as previously described. Although damaged, it is clear the anterior process extended to the level of the anterior margin of the orbit. Posteriorly, the jugal dorsal ramus gently curves, expands dorsoventrally and thins mediolaterally. Based on the original reconstruction (Fig. 1A), which featured a complete jugal and postorbital, the jugal contributed to about half of the posterior orbital margin.

Postorbital. An original photograph shows that the postorbital was complete, but we are unable to locate the element (Fig. 1A). Based on the photograph, the element is dorsoventrally short and anteroposteriorly wide, being almost rectangular in shape and making up half of the posterior orbital margin. The anterodorsal edge tapers to a narrow process.

342 *Parietal*. Both parietals are damaged and missing their anteroventral margins, the left element
343 being better preserved (Figs 3, 5A-D). In dorsal view, the parietals are hour-glass shaped and
344 meet medially, diverging slightly anteriorly. CT scans reveal the dorsomedial margin of the
345 anterior parietal is strongly dorsoventrally expanded in transverse section, the elements
346 contacting each other at a tall midline butt joint; the parietal thins ventrolaterally in transverse
347 section. The articulation of the parietals results in a well-defined sagittal crest (Fig. 5A, C); at its
348 mid-section, the parietal is L-shaped in transverse section with the horizontal leg forming the
349 roof of the braincase while the ventral leg forms the lateral wall of the braincase and medial wall
350 of the supratemporal fenestra. Lateral to the crest, the dorsal surface of the parietal is convex and
351 curves ventrally, widening posteriorly. Posteriorly, the crest decreases in height to form an
352 extensive shelf (parietal ridge) under which the supraoccipital articulates (Fig. 5A, C). Two
353 elongate depressions, one on the posterior aspect of each parietal, may represent attachment sites
354 for epaxial neck muscles (Fig. 5C).

355 In ventral view, the surface of the parietal is concave and bears impressions of structures
356 that surrounded the brain (Fig. 5B, D). In the anterior region, impressions of the cerebral
357 hemisphere and extra-encephalic depression are present (as in McGowan, 1973). McGowan
358 (1973, fig. 48) showed that the cerebral hemisphere was present in both the parietal and frontal in
359 a specimen of *Ichthyosaurus*. In BMT 1955.G35.1, there is no indication of the frontal at this
360 position, suggesting the cerebral hemispheres were likely limited to the parietal. The descending
361 parietal flange is present in both parietals, although the left is more complete (Fig. 5B, D). The
362 anterior process is thick, short, and protrudes forwards, creating a ledge. Towards the center of
363 the parietal is the large, ovoid impression of the optic lobe, the most prominent of the cerebral
364 structures, situated posterior to the parietal flange (Fig. 5B). The epiterygoid process is missing.

Posteriorly, the parietal flares ~~outwards~~ to form the paraoccipital process; in posterior view, this process is shaped like a bowtie and ventrally deflected. In ventral view, there may be an impression of the cerebellum, although this is difficult to confirm because this portion is damaged.

Supratemporal. Portions of both supratemporals are preserved. The majority is exposed at the posterior margin of the skull, attached to the parietal (Figs 3C, 5C). It is difficult to identify the parietal-supratemporal suture in the original specimen. In CT scans, the contact between the left parietal and supratemporal is visible as a very tight, sinuous butt joint; this contact cannot be discerned on the right and the two bones may have fused. In posterior view, the preserved supratemporal is large and triradiate; it is narrow medially and increases in width distolaterally, with a posteroventral process. In this view, it is roughened with numerous striae, probably for muscle attachment (Kirton, 1983) (Fig. 5C). There are also some foramina present, similar to those reported in this region of the supratemporal in ichthyosaurs such as the Cretaceous *Leninia stellans* (Fischer et al., 2014).

Anatomical description of the palate

The left pterygoid, including a fragment representing the quadrate wing, and quadrate are preserved (Fig. 3).

Pterygoid. The left pterygoid can be positively identified, although it is damaged. It is an anteroposteriorly elongate element with a robust and mediolaterally wide posterior end and narrow anterior end (palatal ramus) (Figs 3, 5E-F). The palatal ramus is dorsoventrally flattened and makes up over half the length of the pterygoid; it is narrowest at its mid-length and expands

388 distally. Posteriorly, the pterygoid expands mediolaterally and dorsoventrally to form the
389 quadrate ramus; its dorsal surface rises in a ridge that would have been continuous with the
390 quadrate wing (see below). The general morphology of the pterygoid is more similar to that of
391 *Sveltonectes* (Fischer et al., 2011, fig. 2G) than *Ophthalmosaurus* (Moon & Kirton, 2016, plate.
392 6, figs 1, 2).
393 In dorsal view, the posterior end has three wing-like projections. The medial projection,
394 which is damaged and was originally more extensive, is the largest and most robust, whereas the
395 lateral projection is slender and dorsoventrally flattened (Fig. 5E). The ventral surface is better
396 preserved, although the edge of the interpterygoid vacuity is damaged (Fig. 5F). Regardless, the
397 posterior end of the pterygoid is larger, wider, and narrows more gradually than that of
398 *Ichthyosaurus* (McGowan, 1973, fig. 20B). The dorsal (quadrate) wing of the posterior ramus of
399 the left pterygoid is almost certainly represented by a large but thin fragment of bone, the shape
400 of which was obscured by a large amount of wood and plaster in the original reconstruction but
401 is revealed in CT scans.
402
403 *Quadrate*. Only the left quadrate is preserved, which is a large and robust element (Figs 3, 5G-I).
404 In anterior and posterior views the quadrate is C-shaped, owing to strong curvature of the shaft
405 (Fig. 5G-H). The articular condyle is massive and greatly expanded mediolaterally, whereas the
406 dorsal end is mediolaterally thin. A well-defined ridge is present above the condyle and displays
407 a long groove identified as the quadratojugal facet. A groove is present on the ventral surface of
408 the condyle, dividing the jaw joint surface into two distinct faces. Fischer et al., (2012, pg. 9),
409 reported a similar groove in the Early Cretaceous ophthalmosaurid *Acamptonectes*.
410

411 *Anatomical description of the braincase*

412 Preserved material includes the supraoccipital, left opisthotic, left stapes, and parabasisphenoid
413 (Fig. 3). The anterior portion of the parasphenoid as well as the basioccipital, prootics, and
414 exoccipitals are missing.

415 *Supraoccipital*. The median supraoccipital is triangular with its apex anterodorsally directed
416 (Fig. 6A-C). CT scans revealed that the right margin of the supraoccipital had been reconstructed
417 in plaster, obscuring the true shape of this element. In anterior and posterior views, the element is
418 convex and arch-like, and is wider than it is tall. A median ridge is present on the posterior
419 surface, which is sharpest anterodorsally and flattens as it approaches the foramen magnum (Fig.
420 6B-C). This ridge would have contacted the parietal, as shown in the 3D model (Fig. 3C, F) and
421 separates two flat, posterolaterally-directed faces, each of which is pierced by a canal that opens
422 onto its internal surface (Fig. 3B, G). These openings probably represent the foramen
423 endolymphaticum (Andrews, 1910), which served for the passage of the endolymphatic ducts
424 (McGowan, 1973; Maisch, 2002; Marek et al., 2015) or veins (Kirton, 1983; Moon & Kirton,
425 2016). The complete left half preserves two articulation facets along its ventrolateral margin – a
426 larger, posteroventrally-directed facet that is deep and triangular-shaped (apex pointing forward)
427 and a smaller, oval-shaped facet that is posterolaterally-directed.

428 In dorsal view, there is a well-defined ridge that is separated by a long, trenchant groove
429 (Fig. 6B). For *Ichthyosaurus*, McGowan (1973, pg. 15) described the dorsal edge as having two
430 shallow grooves. The groove marks the boundary between the ossified and cartilaginous portions
431 of the neurocranium (McGowan, 1973). In ventral view, the element is arched with a smooth
432 section for the roof of the foramen magnum (Fig. 6C). The exoccipital facet is roughly square.
433

434 *Parabasisphenoid*. The thin parasphenoid is broken with a small portion preserved fused to the
435 basisphenoid (Fig. 6D). The basisphenoid is complete and is a large, robust element both
436 mediolaterally wide and dorsoventrally tall (Fig. 6D-E). There are deep grooves between the
437 posterior corners of the bases of the basipterygoid processes and the main body for the palatal
438 ramus of the facial nerve (Kirton, 1983). In dorsal view, the midline of the anterior end is convex
439 and, along with the protruding anterior ends of the basipterygoid processes, gives the anterior
440 margin of the basisphenoid a 'three-pronged' appearance, resembling a specimen of
441 *Ichthyosaurus* referred to as the 'Evans Nodule' by McGowan (1973, plate 1a). The
442 basipterygoid processes are both complete, robust and oblong in ventral view (Fig. 6E). Their
443 surfaces appear slightly roughened, probably due to a cartilaginous covering for contact with the
444 pterygoid. The distal articular facet of the basipterygoid process is defined by a depression with a
445 rim. The anterior tip of the basipterygoid process is tapered, whereas the posterior margin is
446 thickened and rounded.
447 The anterodorsal aspect of the basisphenoid features a pair of robust protuberances
448 separated by a slight midline depression – the sella turcica – that housed the pituitary gland (Fig.
449 6D). Below this is the median opening for the carotid artery, which courses posteroventrally
450 through the bone and exits on its ventral surface as a rounded opening bounded proximally by an
451 arch-like ridge (Fig. 6D-E). Ventral to this opening and dorsal to the parasphenoid is a kidney-
452 shaped articulation facet, interpreted as the impressions of paired trabeculae (as in McGowan,
453 1973, fig. 1) (Fig. 6D). Immediately dorsal and posterior to the sella turcica, is a large, bulbous
454 region that has the ossified dorsum sellae (dorsal crest). The posterior surface is a wide, rounded
455 rectangle, indented for reception of the basioccipital.
456

457 *Opisthotic*. Only the left opisthotic could be identified (Fig. 6F-G). It is a robust and stout
458 element that is roughly pentagonal in posterior view. Its ventrolateral margin is long and sharp.
459 Ventrally the opisthotic tapers to a point that bears a small facet, which articulates with the
460 stapes. The stapedial facet is large, but the lateral 'foot' (after Fischer et al., 2012) has minor
461 exposure. The ventromedial margin is concave and bears a long, low groove that marks the
462 basioccipital facet (Fig. 6G). The dorsolateral margin forms the prominent paroccipital process,
463 the posterior surface of which bears a long, prominent ridge that ascends vertically from the
464 ventral tip of the element, then turns medially. A deep groove, for either the glossopharyngeal or
465 branch of the facial nerve (Kirton 1983; Marek et al., 2015), separates this ridge from a
466 pronounced protuberance on the dorsal margin of the opisthotic. The dorsomedial margin is
467 expanded into a rugose, subtriangular depression (apex pointing posterodorsally) surrounded by
468 a raised lip and several small protuberances. Although poorly preserved, the membranous
469 impressions of the posterior vertical semicircular canal, sacculus, the horizontal semicircular
470 canal and possibly utriculus are represented by a somewhat 'V-shaped' impression, best
471 observed in anteromedial aspect (Fig. 6F). The impression of the horizontal semicircular canal is
472 damaged at the tip and the impression of the sacculus is wide and round. There are several
473 grooves positioned adjacent to the impressions, which McGowan (1973, fig. 5) referred to as
474 grooves in the margin circumscribing the membranous impression. Computed tomography
475 reveals a great deal of trabecular bone within the opisthotic.
476
477 *Stapes*. Both stapes are preserved, with the left being more complete. The stapes is
478 mediolaterally elongate with a bulbous occipital head and a tapered distal end (Fig. 6H). The
479 proximodorsal region of the medial head bears a groove that marks the course of the stapedial

artery. In anterior view, the medial head is laterally inclined and there is a shallow groove, which is probably the opisthotic facet. The posterior surface of the stapes bears a series of oblique ridges and grooves. This may have been an area for muscle attachment (McGowan, 1973, fig. 7a) (Fig. 6H). There are several small canals within the stapes; however, these are very difficult to trace.

Anatomical description of the lower jaw

Nearly complete left and right dentaries are present, as are both incomplete splenials, the nearly complete left surangular, and the complete left articular and angular (Fig. 4).

Dentary. The dentary makes up over three-quarters the length of the lower jaw. It is elongate, tapering at its anterior and posterior ends (Figs 1, 4). The ventral margin is convex while the dorsal margin is concave, and the entire element curves dorsally at its anterior end; the latter is likely the result of taphonomic distortion. As with the upper jaw, the lower teeth have been reset in a continuous groove, which we use as landmarks for our description. In transverse section, the anterior dentary is roughly oval-shaped with a convex lateral surface; a medial shelf forms the floor of the alveolar groove and a dorsal lamina laterally overlaps the dentary teeth. The medial shelf is separated from a longitudinal ridge that parallels the ventral margin of the bone by a shallow groove (lateral wall of the Meckelian canal); this ridge and groove dominate the internal face of the anterior half of the dentary. At the level of the 15th dentary tooth, the medial shelf disappears and the dentary becomes a laterally bowed sheet of bone with a thickened dorsal margin in transverse section.

The anterior tip of the right dentary is damaged and, as a result, the dentaries do not contact each other anteriorly to form the mandibular symphysis (Figs 1, 4). As preserved, the dentary and splenial do not contact each other along their entire length but this is due to distortion. The anterior tip of the angular is level with the 17th preserved tooth on the right side; the angular laterally overlaps the ventral margin of the dentary in a very tight scarf joint. In contrast, the suture between the dentary and surangular, which reaches the level of the 22nd preserved dentary tooth, is a loose, horizontal butt joint except at its posterior end where the posterior tip of the dentary laterally overlaps the surangular.

As with the premaxilla, CT scans reveal that each dentary encloses an elongate, branching canal ventral and lateral to the tooth row that extends from the anterior tip of the bone to the 14th (right) and 9th (left) preserved dentary teeth, at which point the canal opens onto the internal surface (Meckelian canal) of the lower jaw ventral to the medial shelf of the dentary (Fig. 4C, G-J). Anteriorly, four small canals branch laterally from the main conduit and open onto short, posteriorly elongated grooves on the lateral face of the dentary. A posterior (fifth) canal opens into a very long groove ventral and parallel to the tooth row that extends over a quarter the length of the dentary.

Splenial. The splenial is composed of a vertical sheet of bone that is medially concave, a slightly thickened dorsal margin that is turned medially, and a thickened, laterally deflected ventral margin. Thus, the element has a mild S-shape and is mediolaterally thin in transverse section anteriorly, becoming more robust with increasingly pronounced curvature posteriorly. The splenial forms the medial wall and part of the floor of the Meckelian canal for the posterior half of the lower jaw. Its contacts with other elements cannot be reliably interpreted as the bones

were not in articulation; however, from their preserved ventral margins, it appears the splenial and angular met in a butt joint.

Angular. The angular extends over half the length of the lower jaw (Figs 1, 4B). The anterior half of the angular is a long, straight rod while the posterior half is both dorsoventrally and mediolaterally expanded, curving dorsally and medially towards the jaw joint. In transverse section, the anterior half of the angular is diamond-shaped with a dorsomedial surface that contacts the ventral margin of the dentary in a tight scarf joint and a dorsolateral surface that meets the ventral margin of the surangular in a loose butt joint. The ventromedial surface of the anterior angular bears a shallow, longitudinal groove bounded dorsally and ventrally by low ridges that presumably articulated with the splenial. Posteriorly, the angular develops a robust tab or lamina that extends from its dorsomedial surface and medially laps the surangular. However, immediately ventral to the jaw joint, this lamina disappears and is replaced by taller, mediolaterally thin dorsolateral lamina that extensively overlaps the lateral aspect of the posterior surangular. Thus, the contact between the angular and surangular is morphologically simple and loose anteriorly but tighter and more complex posteriorly. In lateral view, the anterior end of the surangular is broken and it appears the angular extends further anteriorly than the surangular (Fig. 4B). This is similar to specimen SOMAG 12, a referred specimen of *Protoichthyosaurus prostaxalis* (Lomax, Massare & Mistry, 2017).

Surangular. The surangular is a long, curved element forming the lateral aspect of the posterior third of the lower jaw (Figs 1, 4B). The anterior half of the surangular is poorly preserved as it is mediolaterally thin and is loosely joined to the dentary (dorsally) and angular (ventrally) via

548 rounded butt joints. Posterior to the dentary, the dorsal margin of the surangular thickens
549 dramatically to form the peaked coronoid process. A longitudinal lateral ridge, dorsally bounding
550 the fossa surangularis, continues to the end of the surangular and separates the thickened dorsal
551 margin from the thinner ventral lamina that articulates with the angular. The element expands
552 dorsally and medially at its rounded posterior end to laterally cup the articular.
553 In medial view, the posterior surangular bears a ridge parallel to its ventral margin that
554 articulates with the angular and forms the floor of the adductor fossa. There is another, more
555 robust ridge on the medial surface originating at the coronoid process and widening posteriorly
556 to contact the anterior surface of the articular. The medial face of the surangular between the two
557 ridges is concave and forms the Meckelian groove and lateral wall of the adductor fossa. There is
558 a large foramen clearly visible on the medial aspect ventral to the coronoid process; this foramen
559 passes laterally through the surangular and exits ventral to the ridge on the lateral surface (Fig.
560 4C, K).
561
562 *Articular*. The preserved left articular has a triangular profile in dorsal and ventral views, with
563 the apex posteriorly and medially directed, and a subcircular profile in medial and lateral views.
564 The posterior margin is sharp while the anterior aspect is flat and broad where it contacts the
565 quadrate to form the jaw joint. The medial aspect of the bone is smooth while the lateral aspect is
566 pitted and porous. CT scans reveal several small, short canals that penetrate into the bone from
567 its lateral surface.
568
569 *Hyoid*. Both hyoids are preserved and are large and complete, although some damage is
570 apparent. The hyoid is a curved, rod-like bone (Fig. 5J). In dorsal view, the element is slightly

bowed posterolaterally and the center of the element is slightly mediolaterally narrower than either end. The anterior end is slightly flattened, rounded and pitted for reception of cartilage. In anterior view, the probable left hyoid is oval-shaped, with a defined rim.

Dentition. The teeth were implanted in an aulacodont fashion in continuous alveolar grooves as is typical in ichthyosaurs. As previously mentioned, the teeth were not preserved in situ and were added to the grooves during reconstruction of the skull both in 1955 and in 2015; thus, they are not in their original positions. Furthermore, the dental groove is too poorly preserved to determine the exact number of teeth that would have originally been present. There are additional fragmentary and complete teeth associated with the specimen.

The teeth are lingually curved, large cones with short, robust crowns with fine striations and smooth apices (Figs 1B-C, 5K). In complete teeth, the crown is much narrower than the root. The roots are large with prominent longitudinal grooves that extend to the base of the crown and continue as longitudinal striations on the crown (Fig. 5K). This morphology is found in all specimens of *Protoichthyosaurus* that have well-preserved teeth (Lomax, Massare & Mistry, 2017; Lomax & Massare, 2018). Tooth morphology for each tooth is similar, with crowns ranging from 0.87 cm to 1.75 cm in height. As no teeth were preserved in situ, it is impossible to differentiate between the premaxillary, maxillary and dentary teeth. A resorption pit is present on the lingual surface in many teeth (e.g. Fig. 5K). CT scans reveal hollow pulp cavities within the teeth that open at the tooth bases and extend nearly the entire height of the tooth.

Anatomy of the postcranial skeleton.

593 Portions of the vertebral column, ribs, gastralia, forefin, pectoral girdle, pelvic girdle and the
594 hindfin are preserved (Fig. 7). The forefin and hindfin phalangeal elements are entirely free of
595 matrix and are not in their original context, so it is impossible to say whether elements are from
596 the left or right fin.
597
598 *Axial skeleton*. A total of 37 vertebral centra are present, all of which are disarticulated. Most are
599 poorly preserved but their positions in the column can be identified from their morphology. One
600 centrum is unusual in possessing the following features: triangular in anterior and posterior
601 views; being marginally anteroposteriorly longer than the preserved cervicals; diapophyses and
602 parapopthyses being high and positioned at the anterior end of the centrum in lateral view; two
603 separate semi-circular facets for articulation with intercentra in ventral view (Fig. 7A-B). This
604 morphology is indicative of an atlas-axis complex, but the centrum displays no fusion. This is
605 unusual given that, with the possible exception of immature individuals, the atlas-axis is always
606 fused in ichthyosaurs (McGowan & Motani, 2003). The presence of two facets on the ventral
607 surface might suggest that this element is the atlas, with the diagonally-oriented anterior facet
608 being for the atlantal intercentrum and the posterior facet for the axial intercentrum (Fig. 7B).
609 Alternatively, and more likely, this is the axis, with the anterior facet being for the axial
610 intercentrum and the posterior facet being for the intercentrum of the third cervical vertebra
611 (McGowan & Motani, 2003, fig. 5C). Interestingly, the anterior surface of the axis centrum is not
612 well-defined, nor smooth and lacks the convexity typical of ichthyosaur centra (Fig. 7A). This
613 might be pathological or it could be the surface that was fused with the atlas vertebra that is not
614 usually preserved (or exposed). A second centrum features similar morphology but is slightly
615 anteroposteriorly shorter and has only one small, anterior facet on the ventral surface, which

articulates with the aforementioned vertebra. It is likely that this is the centrum of the third cervical vertebra. The remaining vertebral centra include 19 dorsals, including elements from the anterior, middle and posterior portions of the series as identified by their shape and position of the diapophyses and parapopthyses, and 16 caudal vertebra, again including elements from the anterior, middle and posterior portions of the series as identified by their shape and the presence of a single rib facet.

One isolated and damaged neural spine, which is mediolaterally thin at its distal end, is preserved.

Numerous incomplete ribs and rib fragments are preserved. The cross-sectional geometry of the ribs varies, with some being rounded whereas others have a dumbbell-shaped cross section. A possible gastralia fragment is present, which is roughened at its anterior end where it presumably met its counterpart at the midline.

Pectoral girdle. The left coracoid is practically complete (Fig. 7C). It is a robust element that is slightly anteroposteriorly longer than mediolaterally wide (Table 1). It has prominent and well-developed anterior and posterior notches. The anterior notch is wider than the posterior notch, resulting in the posterior end of the coracoid being mediolaterally wider than the anterior end. A prominent rim outlines the glenoid and scapular facets, the former being noticeably longer than the latter. In medial view, the intercoracoid facet is dorsoventrally thickened and bulbous at the anterior end but narrows posteriorly.

Only the left scapula is preserved and is missing its posterior end (Fig. 7D). The anterodorsal end is marked by a right angle, which extends to the ventral edge. This proximal

638 end is twice as tall dorsoventrally as the mid shaft and is widely flared but without a prominent
639 acromion process.
640
641 *Forefin*. As mentioned previously, none of the phalangeal elements were found in articulation. It
642 is impossible to determine whether the elements are from the left or right fin or determine the
643 morphology of the forefin in this specimen. The radius and ulna are missing and the preserved
644 elements are polygonal. Of note, the forefin was reconstructed for display in 1955 and 2015 with
645 the morphology typical of *Ichthyosaurus* (Motani, 1999). This was prior to the resurrection of
646 *Protoichthyosaurus* (Lomax, Massare & Mistry, 2017).
647 A single, nearly complete left humerus is robust, elongate, and slightly wider distally than
648 proximally without a prominent constriction in the mid shaft (Fig. 7E-F). It is the largest
649 humerus of *Protoichthyosaurus* described thus far (Table 1). The proximal end is large, bulky
650 and the surface is rugose and roughened. In ventral view, the deltopectoral crest is offset
651 anteriorly and is large but does not extend far down the shaft. The base of the anterior end is
652 slightly flared due to the presence of an anterior facet. The dorsal process is broken but appeared
653 centrally located. There are several possible predation marks preserved on the ventral surface of
654 the humerus (Fig. 7F). The facets for the radius and ulna are also damaged.
655
656 *Pelvic girdle*. A single ilium is well-preserved (Fig. 7G). It is a relatively thick and elongate
657 element that is J-shaped in lateral and medial views, resembling the ilium of *Ichthyosaurus*
658 *somersetensis* in being more oblong than rib-like (Lomax & Massare, 2017). The presumed
659 posterior end is slightly bulbous, relative to the shaft, somewhat similar to the ilium of
660 *Protoichthyosaurus applebyi* (Lomax, Massare & Mistry, 2017, UNM.G.2017.1). The presumed

anterior end is highly rugose. A possible ischium might also be preserved, but it is heavily damaged.

Hindfin. Like the forefin, some phalanges of the hindfin are preserved, which are largely polygonal, but none were found in articulation and all have lost their original context. Regardless, the single, incomplete femur provides information (Fig. 7H-I). As the proximal end is poorly preserved, it is difficult to identify the element as being from the left or right, but it is most likely a right femur, based on the following comments. It has a very slender shaft, narrow proximal end, and a flared distal end. Both the dorsal and ventral processes are damaged and worn, but the supposed dorsal process seems to be a prominent, narrow ridge and the supposed ventral process is large. There is a slight flare at the anterior end, but the posterior end is only slightly expanded, and is almost a right angle. The tibial facet is larger than the fibular facet.

Historically modelled regions of the skull of BMT 1955.G35.1

CT-scanning the skull of BMT 1955.G35.1 aided substantially in our anatomical description. Additionally, modelled areas of the skull can be clearly differentiated from fossil bone in scans by the differing densities of these materials (Fig. 8). Fossil bone is the densest material (appearing as bright areas within CT scans) followed by regions of the braincase that were 3D printed in gypsum (see Material and Methods). Areas of the skull modelled during its initial reassembly post-May 1955 are the least dense, as they are either composed of wood or a traditional mix of alvar, jute and kaolin (known as AJK dough). Some modelled areas – such as the posterior third of the right lower jaw, central portion of the right jugal, and "symphysis" between left and right dentaries – are immediately apparent. Other areas, including the right

lacrimal and prefrontal, and various patches in the lower jaws, are less obvious. The skillfully modelled right margin of the supraoccipital is only evident in CT scans, as are portions of the braincase that were 3D printed and added to the newly reassembled skull. Thus, our work demonstrates the utility of applying CT scanning to older, potentially modified museum specimens to better understand both anatomy and specimen history.

3D digital reconstruction of the skull of BMT 1955.G35.1

Limits to the data set used in the 3D digital reconstruction of the skull must be noted. Numerous bones are absent, fragmentary or were too delicate to scan, and some aspects of the 3D reconstruction are uncertain. For example, the width of the reconstructed skull is constrained by the articulation of the premaxillae (anteriorly) and contacts between the basisphenoid, pterygoids and quadrate (posteriorly). Bones of the skull roof and palate that determine width in the middle part of the skull are missing. Furthermore, the placement of the preserved bones of the posterior skull roof is an estimate based on 1) the predicted height of the missing exoccipitals relative to other braincase elements, and 2) the assumption of a smooth slope between the nasals and parietals, as observed in other large ichthyosaurs, including examples of the genus *Protoichthyosaurus* (Lomax, Massare & Mistry, 2017; Lomax & Massare, 2018). We did not attempt to retrodeform elements that experienced plastic deformation, specifically the lower jaws. The exaggerated dorsal and lateral curvature of these elements prevents complete closure of the upper and lower jaws in our model. Similarly, the premaxilla and nasals could not be completely re-articulated due to their deformed nature. Thus, this 3D digital reconstruction is our current best hypothesis of the original skull shape of BMT 1955.G35.1 based on preservation and personal interpretation. With these limitations in mind, the digital reconstruction nonetheless

yields useful new information on overall skull shape in this taxon (Fig. 9; Appendix S3). This skull shape is typical of *Protoichthyosaurus prostaxalis* in lateral view (Fig. 9A), in having a low skull that is slightly inclined from the nasals to the posterior end of the skull and in possessing a relatively long and slender rostrum especially when compared with Lomax et al., (2017, figs. 2C, 4A-B) and Lomax and Massare (2018, figs. 2–3).

Due to the limitations of the fragile nature of the specimen some of the bones could not be articulated in life position in the physical model and there are differences between the digital and physical (Figs. 1, 2; Appendix S1) models. Of note, the rear of the skull is mediolaterally wider and dorsoventrally shorter in the digital reconstruction than in the physical model. This is due to placement of the basisphenoid dorsal and anterior to its true articulation with the pterygoids in the physical model, as well as midline contact between the pterygoids; the pterygoids are separated by the basisphenoid in ichthyosaurs (McGowan, 1973, Kirton, 1983; Kear, 2005). The stapes is dorsally displaced in the physical reassembly; in other ichthyosaurs, the stapes contacts the quadrate dorsal to its expanded base (Andrews, 1910; Kirton, 1983; McGowan & Motani, 2003). Lastly, the jugal extends posterior to the quadrate in the physical model, leaving no space for the posterior facial bones and resulting in the upper jaw being anteroposteriorly shorter than the lower jaw. Shifting premaxilla and contacting bones so that the anterior tips of the premaxillae and dentaries are level results in a gap between the jugal and quadrate large enough to accommodate the missing postorbital and quadratojugal. These differences highlight another advantage of applying 3D imaging and visualization methods to large specimens. Large fossil bones are fragile and heavy, and there are practical limitations to how they can be physically manipulated and mounted when reassembling a skull or skeleton;

729 digital manipulation of fossil bones reduces risk to the specimen and errors can be easily
730 corrected.
731

732 Discussion

733 BMT 1955.G35.1 has never formally been described. The original museum record shows that it
734 was initially identified as *Ichthyosaurus communis,* a species to which many ichthyosaur
735 specimens were historically referred as it is the most common and widespread Lower Jurassic
736 ichthyosaur genus in the UK (but see Massare & Lomax, 2017). In notes held at the
737 Warwickshire Geological Records Service (pers. comm. J. Radley, 2015), a report by Dr Brian
738 Seddon, stated: "It is believed that this animal is a new species lying somewhere between
739 communis [*I. communis*] and breviceps [*I. breviceps*]". A 1957 letter from Seddon states that it
740 was Robert Appleby who expressed the opinion that the specimen possibly represented a new
741 species and requested photos be taken. More recently, Larkin et al. (2016) tentatively identified
742 the specimen as *Ichthyosaurus,* based on available information at the time. Since then, a revised
743 diagnosis of *Ichthyosaurus* has been published (Massare & Lomax, 2017), along with a
744 redescription of *Protoichthyosaurus* (Lomax, Massare & Mistry, 2017), a genus first described
745 by Appleby (1979), which was later synonymized with *Ichthyosaurus* (Maisch & Hungerbühler,
746 1997).

747 Lomax et al. (2017) provided an emended diagnosis of *Protoichthyosaurus*, which
748 included several autapomorphies of the forefin. Lomax and Massare (2018) provided additional
749 information on the genus and species, including a revised diagnosis, and showed that the genus
750 can also be distinguished from *Ichthyosaurus* by a combination of skull characters. They further
751 noted that characters used to distinguish individual species of *Protoichthyosaurus* from

individual species of *Ichthyosaurus* are more easily evaluated. The forefin of BMT 1955.G35.1 is entirely reconstructed. We have been unable to locate photographs or illustrations of how the freshly excavated forefin appeared. Thus, the forefin cannot be used to identify the specimen.

BMT 1955.G35.1 does possess genus features shared by both *Ichthyosaurus* and *Protoichthyosaurus*, including: a coracoid with both prominent anterior and posterior notches; scapula with a narrow shaft that is expanded at the anterior end, but without a prominent acromion process; a humerus with nearly equal width distally and proximally, with only a slight constriction in the shaft; and femur longer than wide, with distal end wider than proximal end. BMT 1955.G35.1 can, however, be assigned to *Protoichthyosaurus* on the basis of several characters. Some of these characters are also found in some species of *Ichthyosaurus* but not in the same combination (Lomax & Massare, 2018). They include: the prefrontal anterior process separates the lacrimal dorsal process from the anterior orbit margin; strongly asymmetric maxilla with long, slender anterior process; teeth that have large roots with deep, prominent grooves that extend to the base of the crown and are continuous with the ornamentation of the crown itself; and a long, slender rostrum. In addition, the slightly diverging anterior end of the parietals in BMT 1955.G35.1, which leaves an opening at the anterior end, is indicative of the posterior opening for the pineal foramen between the parietals and frontals. Because the frontals are not preserved, it is not possible to confirm if this is correct, but it seems plausible as this is the position of the pineal in *Protoichthyosaurus* (Lomax & Massare, 2018). In *Ichthyosaurus* the pineal is between the frontals and parietals (Massare & Lomax, 2017).

Protoichthyosaurus prostaxalis and *P. applebyi* differ in skull and humeral morphologies (Lomax, Massare & Mistry, 2017). A third questionable species, *P. fortimanus*, known only from an isolated forefin missing the humerus, displays only characters of the genus (see discussion in

Lomax & Massare, 2018). The left humerus of BMT 1955.G35.1 is damaged on its dorsal surface. This restricts its usefulness in identification because the two species can be differentiated by the dorsal process, which is missing in this specimen. The humerus of BMT 1955.G35.1 is robust, more similar to *P. prostaxalis* than *P. applebyi*, but this may be due to the large size of BMT 1955.G35.1 (see Lomax, Massare & Mistry, 2017, fig. 5). However, considering the size, Lomax and Massare (2018) described only the second known specimen of *P. applebyi*, an isolated skull (NHMUK R1164), which is comparable in size with some smaller specimens of *P. prostaxalis*. They identified NHMUK R1164 as probably an adult and showed that the differences among the two species are not ontogenetic. BMT 1955.G35.1 is more than twice the size of NHMUK R1164 and is probably an adult *P. prostaxalis*. Unfortunately, BMT 1955.G35.1 is missing some features of the skull that distinguish the two species. However, the maxilla of BMT 1955.G35.1 is large, triangular, dorsoventrally high, and possesses a long and narrow anterior process that is longer than the posterior process. In *P. applebyi*, the maxilla is dorsoventrally low. Furthermore, although the jugal is currently incomplete and the postorbital is missing, they were complete and part of the original mount (Fig. 1A). The morphology of the postorbital, in being dorsoventrally short but anteroposteriorly wide almost rectangular, and making up half of the posterior orbit margin are characters found in *P. prostaxalis* (Lomax, Massare & Mistry, 2017; Lomax & Massare, 2018). In *P. applebyi*, the postorbital is dorsoventrally long, anteroposteriorly narrow, and makes up much more than half of the orbit posterior margin (Lomax & Massare, 2018). Thus, based on the morphology and extent of the maxilla and postorbital, we assign the studied specimen to *P. prostaxalis*. The difference in size between the studied specimen and the presumed adult specimen (NHMUK R1164) of *P. applebyi* is another indicator that the studied specimen belongs to *P. prostaxalis*.

798 The maxilla of BMT 1955.G35.1, although dorsoventrally high, does not appear as tall as
799 in some specimens of *P. prostaxalis* (e.g. BRLSI 3555, BU 5323), but this is due to damage to
800 the dorsal lamina of the maxilla on both sides. Alternatively, it may also appear shorter due to
801 the length of the studied skull, which is almost twice that of the largest known specimen of *P.*
802 *prostaxalis* (Lomax, Massare & Mistry, 2017; Lomax & Massare, 2018), with an estimated total
803 skull length of at least 80 cm and estimated mandible length of 87 cm. This is also much larger
804 than the sister taxon *Ichthyosaurus*, with maximum skull and mandible lengths of 57.5 cm and
805 67 cm respectively (Lomax & Sachs, 2017). Considering that the skull length is 20-25% of the
806 total body length, we estimate BMT 1955.G35.1 would have been between 3.2 and 4 m in
807 length. This is the largest example of the genus known, the previous total length estimate of the
808 species being 2.5 m (Lomax, Massare & Mistry, 2017).
809

810 Conclusions

811 In this article, we describe a large, partial ichthyosaur skeleton from the Early Jurassic of
812 Warwickshire. In addition to examining the specimen, we carried out CT scanning of individual
813 skull bones as well as the entire, reassembled skull, one of the first times the skull of a large
814 marine reptile has been successfully CT-scanned, visualized and reconstructed in 3D (see
815 McGowan, 1989; Foffa et al., 2014). CT scanning contributed greatly to our anatomical
816 description by revealing features not visible on original fossil material such as: branching,
817 longitudinal vascular canals within the premaxilla and dentary; short canals penetrating the nasal,
818 lacrimal, stapes, and articular; trabecular bone within the opisthotic; canals in the basisphenoid
819 and supraoccipital; the presence of the quadrate process of the pterygoid; and the sutural
820 morphology. We also demonstrate the utility of applying medical imaging techniques to historic

specimens to differentiate between original fossil material and reconstructed regions, as well as the advantage of using digital visualization to accurately reconstruct large fossil specimens in 3D.

Our study has found additional characters that may lend additional support for the distinction of *Protoichthyosaurus* from its sister taxon *Ichthyosaurus*, such as the morphology of the pterygoid and anteroventral surface of the parietal, which differ from that described for *Ichthyosaurus* (McGowan, 1973). However, considering that only a couple of specimens expose these elements, it is possible that the differences may be the result of individual variation; more specimens of both taxa are needed to test and clarify these findings.

Based on a unique combination of characters, we identify the specimen as *Protoichthyosaurus prostaxalis.* With a skull nearly twice as long as any previously described specimen of *P. prostaxalis,* this specimen greatly increases the known size range of this genus. Compared with known, contemporaneous Sinemurian ichthyosaurs, the estimated size suggests it was larger than all species of *Ichthyosaurus* (Lomax & Sachs, 2017), and comparable with the largest known specimens of *Leptonectes tenuirostris* (McGowan, 1996a), but smaller than *Leptonectes solei* (McGowan, 1993), *Excalibosaurus costini* (McGowan, 2003) and *Temnodontosaurus platyodon* (McGowan, 1996b). Thus, our study also provides new information on ichthyosaur diversity and potential ecology in the Early Jurassic of the UK.

Acknowledgements

Firstly, we would like to thank Luanne Meehitiya (formerly of TSM) who first discussed BMT 1955.G35.1 with NRL and DRL, and provided access to study the specimen. Funding for the conservation work, CT scanning, rebuilding of the skull and redisplay was received from:

844 PRISM fund, Arts Council, England; The Dorothy and Edward Cadbury Trust; The Curry Fund
845 of the Geologists' Association; and internal funding from the Birmingham Museums Trust. We
846 would like to express our thanks to each of the funders, which led to the scientific study and
847 description of the specimen. We also thank Lukas Large (TSM) for assistance and the
848 Birmingham Museums Trust for the photos reproduced in Figure 1B and 1C. Judy Massare and
849 Valentin Fischer are acknowledged for helpful comments on the morphology of the skull. Jon
850 Radley provided information on the geology of the site and records relating to the excavation.
851 David Ward identified the shark tooth and provided stratigraphic information about the species.
852 Michael Howarth identified the ammonite associated with the postcranial skeleton and the
853 ammonites recently collected by NRL from the original site. The current landowner R. E Morley
854 and the tenant farmer Robert Heath gave permission for large holes to be dug at the site and
855 Malcolm Bryan and Sally Bryan (son and wife of the original finder of the specimen, Michael
856 Bryan) and Clive Jeffries assisted with the fieldwork. Ian Boomer (University of Birmingham)
857 analyzed the matrix from the site for microfossils. Robert Asher and Colin Shaw (University of
858 Cambridge) provided access to microCT-scanning facilities; Renate Weller (Royal Veterinary
859 College) carried out CT-scanning of the full skull. Technical support for Avizo was provided by
860 Alejandra Sánchez-Eróstegui and Jean Luc-Garnier (Thermo Fisher Scientific). Steven Dey
861 (ThinkSee3D) mirrored microCT data and 3D printed the missing bones on the right side of the
862 skull. DRL's travel was covered in part by a PGR, Dean's Doctoral Scholarship Award from the
863 University of Manchester.

864

865 ## Author contributions

DRL conceived the project, assisted in disassembling the original skull and reassembling the new skull mount, wrote the first draft of the manuscript, interpreted the morphology from the CT data and created several figures; LBP collected, segmented, visualized and interpreted CT data, created several figures, helped to write the manuscript and created the 3D PDFs; NRL conceived the project with DRL, cleaned, conserved and prepared the specimen, disassembled the original skull and rebuilt it more accurately, located the postcranial skeleton and visited the original site of discovery to collect more data. DRL, LBP and NRL described the specimen and wrote the manuscript. All authors gave final approval for publication.

Data archiving statement

Data for this study are available in…

Supporting information

Additional Supporting Information can be found in the online version of this article:

Appendix S1. 3D PDF of segmented CT scans of the reassembled skull of *Protoichthyosaurus prostaxalis* (BMT 1955.G35.1). Download the PDF file and click once on the skull to activate. Left-click to rotate the model; right-click to zoom in or out; and hold both buttons to pan. Check or uncheck boxes in the model tree in the upper left corner of the viewer to display or hide individual parts.

Appendix S2. Transformation matrices for the 3D digital reconstruction of *Protoichthyosaurus prostaxalis* (BMT 1955.G35.1) from original CT data.

Appendix S3. 3D PDF of the reconstructed skull of *Protoichthyosaurus prostaxalis* (BMT 1955.G35.1).

889

890 ## References

891 Andrew, CW. 1910. *A descriptive catalogue of the marine reptiles of the Oxford Clay. Part I.*
892 British Museum (Natural History), London, 205 pp.

893 Appleby RM. 1979. The affinities of Liassic and later ichthyosaurs. *Palaeontology* **22**:921–946.

894 Benton MJ, Spencer PS. 1995. Fossil Reptiles of Great Britain. Chapman and Hall, London, 386
895 pp.

896 Benton MJ, Taylor MA. 1984. Marine reptiles from the Upper Lias (Lower Toarcian, Lower
897 Jurassic) of the Yorkshire coast. *Proceedings of the Yorkshire Geological Society* **44**:399-429.

898 Bonaparte CL. 1841. A new systematic arrangement of vertebrated animals. *Transactions of the*
899 *Linnean Society of London* **18**:247-304.

900 Button D, Barrett P, Rayfield E. 2016. Comparative cranial myology and biomechanics of
901 *Plateosaurus* and *Camarasaurus* and evolution of the sauropod feeding apparatus.
902 *Palaeontology* **59**:887-913.

903 Cox P, Rinderknecht A, Blanco R. 2015. Predicting bite force and cranial biomechanics in the
904 largest fossil rodent using finite element analysis. *Journal of Anatomy* **226**:215-223.

905 De Blainville HD. 1835. Description de quelques espèces de reptile de la Californie, précédée de
906 l'analyse d'un système general d'Erpétologie et d'Amphibiologie. *Nouvelles*
907 *Annales du Muséum d'Histoire Naturelle* **4**:233-295.

908 Delair JB. 1969. A history of the early discoveries of Liassic ichthyosaurs in Dorset and
909 Somerset (1779–1835). *Proceedings of the Dorset Natural History and Archaeological Society*
910 **90**:1-9.

911 Edmonds EA, Poole EG, Wilson V. 1965. Geology of the country around Banbury and Edge
912 Hill: (explanation sheet 201, new series). HMSO.
913 Fernández M, Carabajal A, Gasparini Z, Diaz G. 2011. A metriorhynchid crocodyliform
914 braincase from northern Chile. *Journal of Vertebrate Paleontology* **31**:369–377.
915 Fischer V, Masure E, Arkhangelsky MS, Godefroit P. 2011. A New Barremian (Early
916 Cretaceous) ichthyosaur from western Russia. *Journal of Vertebrate Paleontology* **31**:1010-
917 1025.
918 Fischer V, Maisch MW, Naish D, Kosma R, Liston J. 2012. New ophthalmosaurid ichthyosaurs
919 from the European Lower Cretaceous demonstrate extensive ichthyosaur survival across the
920 Jurassic-Cretaceous boundary. *PLoS ONE* **7**:e29234.
921 Fischer V, Arkhangelsky MS, Uspensky GN, Stenshin IM. 2014. A new Lower Cretaceous
922 ichthyosaur from Russia reveals skull shape conservatism within Ophthalmosaurinae. *Geological*
923 *Magazine* **151**:60-70.
924 Foffa D, Cuff A, Sassoon J, Rayfield E, Mavrogordato M, Benton M. 2014. Functional anatomy
925 and feeding biomechanics of a giant Upper Jurassic pliosaur (Reptilia: Sauropterygia) from
926 Weymouth Bay, Dorset, UK. *Journal of Anatomy* **225**:209-219.
927 Herrera Y, Fernández M, Gaspirini Z. 2013. The snout of *Cricosaurus araucanensis:* a case
928 study in novel anatomy of the nasal region of metriorhynchids. *Lethaia* **46**:331-340.
929 Jasinoski S, Rayfield E, Chinsamy A. 2009. Comparative feeding biomechanics of *Lystrosaurus*
930 and the generalized dicynodont *Oudenodon. Anatomical Record* **292**:862-874.
931 Kear B. 2005. Cranial morphology of *Platypterygius longmani* Wade, 1990 (Reptilia:
932 Ichthyosauria) from the Lower Cretaceous of Australia. *Zoological Journal of the Linnean*
933 *Society* **145**:583-622.

Kirton AM. 1983. A review of British Upper Jurassic ichthyosaurs. Unpublished PhD thesis, University of Newcastleupon-Tyne, 239 pp.

Larkin NR, Lomax DR, Meehitiya L, Dey S. 2016. The discovery in a museum collection of the largest known skeleton of *Ichthyosaurus* in the world and its re-display, including 3D-printing missing bones. The Annual Symposium of Vertebrate Palaeontology and Comparative Anatomy. Vol 64, p. 12.

Larkin NR, O'Connor S, Parsons D. 2010. The virtual and physical preparation of the Collard plesiosaur from Bridgwater Bay, Somerset, UK. *The Geological Curator* **9**:107-116.

Lautenschlager S. 2016. Reconstructing the past: methods and techniques for the digital restoration of fossils. *Royal Society Open Science* **3**:doi: 10.1098/rsos.160342.

Lautenschlager S, Witmer L, Aaltangerel P, Zanno L, Rayfield E. 2014. Cranial anatomy of *Erlikosaurus andrewsi* (Dinosauria, Therizinosauria): new insights based on digital reconstruction. *Journal of Vertebrate Paleontology* **34**:1263-1291.

Lautenschlager S, Brassey C, Button D, Barrett P. 2016. Decoupled form and function in disparate herbivorous dinosaur clades. *Scientific Reports* **6**:26495. doi: 10.1038/srep26495.

Lautenschlager S, Gill P, Luo Z, Fagan M, Rayfield E. 2017. Morphological evolution of the mammalian jaw adductor complex. *Biological Reviews* **92**:1910-1940.

Lomax DR, Gibson BJA. 2015. The first definitive occurrence of *Ichthyosaurus* and *Temnodontosaurus* (Reptilia: Ichthyosauria) in Nottinghamshire, England and a review of ichthyosaur specimens from the county. *Proceedings of the Geologists' Association* **126**:554-563.

Lomax DR, Massare JA. 2017. Two new species of *Ichthyosaurus* from the lowermost Jurassic (Hettangian) of Somerset, England. *Papers in Palaeontology* **3**:1-20.

957 Lomax DR, Massare JA. 2018. A second specimen of *Protoichthyosaurus applebyi* (Reptilia:
958 Ichthyosauria) and additional information on the genus and species. *Paludicola* **11**:164-178.
959 Lomax DR, Massare JA, Mistry R. 2017. The taxonomic utility of forefin morphology in Lower
960 Jurassic ichthyosaurs: *Protoichthyosaurus* and *Ichthyosaurus*. *Journal of Vertebrate*
961 *Paleontology* **37**:DOI: 10.1080/02724634.2017.1361433.
962 Lomax DR, Sachs S. 2017. On the largest *Ichthyosaurus*: A new specimen of *Ichthyosaurus*
963 *somersetensis* containing an embryo. *Acta Palaeontologica Polonica* **62**:575-584.
964 Lomax DR, De La Salle P, Massare JA, Gallois R. 2018. A giant Late Triassic ichthyosaur from
965 the UK and a reinterpretation of the Aust Cliff 'dinosaurian' bones. *PLoS ONE* **13**:e0194742.
966 Maisch MW, Hungerbühler A. 1997. Revision of *Temnodontosaurus nuertingensis* (v. Huene,
967 1931), a large ichthyosaur from the Lower Pliensbachian (Lower Jurassic) of Nurtingen, South
968 Western Germany. *Stuttgarter Beiträge zur Naturkunde Serie B* **248**:1-11.
969 Maisch MW. 2002. A braincase of *Temnodontosaurus* cf. *trigonodon* (von Theodori, 1843)
970 (Ichthyosauria) from the Lower Jurassic of Germany. *Geologica et Palaeontololgica* **36**:115-122.
971 Marek R, Moon B, Williams M, Benton M. 2015. The skull and endocranium of a Lower
972 Jurassic ichthyosaur based on digital reconstructions. *Palaeontology* **58**:723-742.
973 Martin JE, Frey E, Riess J. 1986. Soft-tissue preservation in ichthyosaurs and a stratigraphic
974 review of the Lower Hettangian of Barrow-upon-Soar, Leicestershire. *Transactions of the*
975 *Leicestershire Literary & Philosophical Society* **80**:58-72.
976 Massare JA, Lomax DR. 2017. A taxonomic reassessment of *Ichthyosaurus communis* and *I.*
977 *intermedius* and a revised diagnosis for the genus. *Journal of Systematic Palaeontology* **16**:263-
978 277.

McGowan C. 1973. The cranial morphology of the Lower Liassic latipinnate ichthyosaurs of England. *Bulletin of the British Museum (Natural History) Geology* **24**: 1-109.

McGowan C. 1989. Computed tomography reveals further details of *Excalibosaurus,* a putative ancestor for the swordfish-like ichthyosaur *Eurhinosaurus. Journal of Vertebrate Paleontology* **9**:269-281.

McGowan C. 1993. A new species of large, long-snouted ichthyosaur from the English lower Lias. *Canadian Journal of Earth Sciences* **30**:1197-1204.

McGowan C. 1996a. The taxonomic status of *Leptopterygius* Huene, 1922 (Reptilia: Ichthyosauria). *Canadian Journal of Earth Sciences* **33**:439-443.

McGowan C. 1996b. Giant ichthyosaurs of the Early Jurassic. *Canadian Journal of Earth Sciences* **33**:1011-1021.

McGowan C. 2003. A new specimen of *Excalibosaurus* from the English Lower Jurassic. *Journal of Vertebrate Paleontology* **23**:950-956.

McGowan C, Motani R. 2003. Handbook of Paleoherpetology, Part 8 Ichthyopterygia. Verlag Dr. Friedrich Pfeil pp. 175.

Milner AC, Walsh S. 2010. Reptiles. In: Lord, A.R., Davis, P.G. (Eds.), Fossils from the Lower Lias of the Dorset Coast. The Palaeontological Association, pp. 372–394.

Moon BC, Kirton AM. 2016. Ichthyosaurs of the British Middle and Upper Jurassic. Part 1 - *Ophthalmosaurus*. *Monograph of the Palaeontographical Society* **170**:1-84.

Motani R. 1999. On the evolution and homologies of ichthyopterygian forefins. *Journal of Vertebrate Paleontology* **19**:28-41.

Motani R. 2005. Evolution of fish-shaped reptiles (Reptilia: Ichthyopterygia) in their physical environments and constraints. *Annual Review of Earth and Planetary Sciences*, **33**:395-420.

1002 Motani R. 2009. The evolution of marine reptiles. *Evolution: Education and Outreach* **2**:224-
1003 235.
1004 Neenan J, Scheyer T. 2012. The braincase and inner ear of *Placodus gigas* (Sauropterygia,
1005 Placodontia) – a new reconstruction based on micro-computed tomographic data. *Journal of*
1006 *Vertebrate Paleontology* **32**:1350-1357.
1007 Nicholls EL, Manabe M. 2004. Giant ichthyosaurs of the Triassic—A new species of
1008 *Shonisaurus* from the Pardonet Formation (Norian: Late Triassic) of British Columbia. *Journal*
1009 *of Vertebrate Paleontology* **24**:838–849.
1010 Porro L, Rayfield, E, Clack J. 2015a. Descriptive anatomy and three-dimensional reconstruction
1011 of the skull of the early tetrapod *Acanthostega gunnari* Jarvik, 1952. *PLOS ONE* **10**:e0118882.
1012 doi: 10.1371/journal.pone.0118882.
1013 Porro L, Rayfield E, Clack J. 2015b. Computed tomography, anatomical description and three-
1014 dimensional reconstruction of the lower jaw of *Eusthenopteron foordi* Whiteaves, 1881 from the
1015 Upper Devonian of Canada. *Palaeontology* **58**:1031-1047.
1016 Porro L, Witmer L, Barrett P. 2015c. Digital preparation and osteology of the skull of
1017 *Lesothosaurus diagnosticus* (Ornithischia: Dinosauria). *PeerJ* **3**:e1494. doi: 10.7717/peerj.1494.
1018 Radley JD. 2003. Warwickshire's Jurassic geology: past, present and future. *Mercian Geologist*
1019 **15**:209-218.
1020 Rayfield E, Norman D, Horner C, Horner J, Smith P, Thomason J, Upchurch P. 2001. Cranial
1021 design and function in a large theropod dinosaur. *Nature* **409**:1033-1037.
1022 Sato T, Wu X, Tirabasso A, Bloskie P. 2011. Braincase of a polycotylid plesiosaur (Reptilia:
1023 Sauropterygia) from the Upper Cretaceous of Manitoba, Canada. *Journal of Vertebrate*
1024 *Paleontology* **31**:313–329.

Sharp A. 2014. Three dimensional digital reconstruction of the jaw adductor musculature of the extinct marsupial giant *Diprotodon optatum*. *PeerJ* **2**:e514. doi: 10.7717/peerj.514.

Smith AS, Radley JD. 2007. A marine reptile fauna from the Early Jurassic Saltford Shale (Blue Lias Formation) of central England. *Proceedings of the Yorkshire Geological Society* **56**:253-260.

Williams M, Benton MJ, Ross A. 2015. The Strawberry Bank Lagerstätte reveals insights into Early Jurassic life. *Journal of the Geological Society* **172**:683-692.

Wroe S. 2007. Cranial mechanics compared in extinct marsupial and extant African lions using a finite-element approach. *Journal of Zoology* **4**:332-339.

Figures

Figure 1. Three-dimensional skull of BMT 1955.G35.1, *Protoichthyosaurus prostaxalis*. A, original photograph of the first skull reconstruction (left lateral view) within a couple of years of the 1955 excavation. Note that the prefrontal and postorbital are present, which we have been unable to locate in our study. B, skull in left lateral view, as reconstructed in 2015. C, skull in right lateral view, as reconstructed in 2015. Note the distinctive asymmetric maxilla with long, narrow anterior process. Teeth are not in their original positions. Scale bar represents 20 cm.

Figure 2. Surface models (generated from CT scan data) of preserved bones from the upper jaw of BMT 1955.G35.1, *Protoichthyosaurus prostaxalis*. Right (A) and left (B) lateral views of the cranium. Medial views of the right (C) and left (D) sides of the cranium. Dorsal (E) and ventral (F) views of the cranium. Lateral views of the right (G) and left (H) premaxillae. Dorsal views of

1048 the right (I) and left (J) premaxillae. Posterior (K) view of the upper jaw. Individual bones are
1049 shown in different colors. Bones in G–J are transparent to visualize internal canals (shown in red
1050 opaque). Teeth are not in their original positions. *Abbreviations*: bs, basioccipital; ex,
1051 exoccipital; f?, possible fragment of frontal; j, jugal; l, lacrimal; mx, maxilla; n, nasal; p, parietal;
1052 pf, prefrontal; pmx, premaxilla; pt, pterygoid; q, quadrate; so, supraoccipital; sp, supratemporal;
1053 st, stapes. Scale bars equal 10 cm.
1054
1055 **Figure 3.** Surface models (generated from micro-CT scan data) of preserved palatal and
1056 braincase bones from BMT 1955.G35.1, *Protoichthyosaurus prostaxalis*. Right medial (A) and
1057 left lateral (B) views, dorsal (C) and ventral (D) views, and anterior (E) and posterior (F) views.
1058 Isolated supraoccipital in right anterolateral view (G). Individual bones are shown in different
1059 colors. Supraoccipital in G is transparent to visualize internal canals (shown in red opaque).
1060 *Abbreviations*: bs, basioccipital; ex, exoccipital; f?, probable fragment of upper pterygoid wing;
1061 p, parietal; pt, pterygoid; q, quadrate; se, sella turcica; so, supraoccipital; sp, supratemporal; st,
1062 stapes. Scale bars equal 10 cm, except for (G) which equals 5 cm.
1063
1064 **Figure 4.** Surface models (generated from CT scan data) of preserved bones from the lower jaw
1065 of BMT 1955.G35.1, *Protoichthyosaurus prostaxalis*. Lateral views of the right (A) and left (B)
1066 lower jaws. Medial views of the right (C) and left (D) lower jaws. Dorsal (E) and ventral (F)
1067 views of the both halves of the lower jaws. Lateral views of the right (G) and left (H) dentary.
1068 Ventral views of the right (I) and left (J) dentaries. Lateral oblique (K) view of the left
1069 surangular. Individual bones are shown in different colors. Bones in G–K are transparent to
1070 visualize internal canals (shown in red opaque). Teeth are not in their original positions.

Abbreviations: an, angular; ar, articular, d, dentary; f?, possible surangular fragment; sa, surangular; sp, splenial; spf, splenial fragment. Scale bars equal 10 cm.

Figure 5. Elements of the skull, palate, lower jaw and dentition of BMT 1955.G35.1, *Protoichthyosaurus prostaxalis*. A-D, incomplete and damaged, articulated parietals in dorsal (A), ventral (B), posterior (C) and anterior (D) view. E-F, incomplete and damaged left pterygoid in posterior (E) and ventral (F) view. Note the three wing-like projections in posterior view. G-I, incomplete and damaged left quadrate in anterior (G), posterior (H) and lateral (I) view. J, hyoids in dorsal view. K, practically complete tooth missing the tip of the crown. Note that the root is large with prominent grooves that extend to the base of the crown and continue as longitudinal striations on the crown. *Abbreviations*: ac, articular condyle; (?)ce, impression of cerebellum; ch, impression of cerebral hemisphere; dpf, descending parietal flange; eed, extra-encephalic depression; ocl, occipital lamella; ol, impression of optic lobe; op, elongate openings in the posterior surface of the parietal; par, palatal ramus; ps, parietal shelf (ridge); qf, quadratojugal facet; sc, sagittal crest; spt, supratemporal probably fused with parietals; vs, ventral surface. Scale bars represent 3 cm.

Figure 6. Braincase elements of BMT 1955.G35.1, *Protoichthyosaurus prostaxalis*. A-C, incomplete supraoccipital in posterior (A), dorsal (B) and ventral (C) view. D-E, parabasisphenoid with complete basisphenoid and broken parasphenoid in anterior (D) and ventral (E) view. F-G, left opisthotic in anteromedial (F) and ventrolateral (G) view. Note the 'V-shaped' membranous impression in F. H, incomplete left stapes in posterior view. *Abbreviations*: bf, facet for basipterygoid facet; bof, basioccipital facet; bp, basipterygoid process; cf, carotid

foramen; ds, dorsum sellae; ef, exoccipital facet; hsc, horizontal semicircular canal; (?)ma, muscle attachment; mh, medial head; mr, median ridge; p, base of parasphenoid; pp, paroccipital process; pvsc, posterior vertical semicircular canal; rfm, roof of foramen magnum; sac, sacculus; sf, stapedial facet; st, sella turcica; t, paired trabeculae; tg, trenchant groove; (?)ut, utriculus. Scale bars represent 3 cm.

Figure 7. Elements of the postcranial skeleton of BMT 1955.G35.1, *Protoichthyosaurus prostaxalis*. A-B, probable 'unfused' (see text for details) axis vertebra in anterior (A) and ventral (B) view. Note the unusual, almost rugose anterior surface. The dark, circular element to the right is a poorly preserved bivalve mollusk. C, left coracoid in dorsal view. D, incomplete left scapula in lateral view. E-F, left humerus in dorsal (E) and ventral (F) view. Note that the dorsal process (trochanter dorsalis) is damaged, as is the facet for the ulna. G, complete ilium in either lateral or medial view. Note that the posterior end (to the right) is bulbous, relative to the shaft. H-I, damaged (?)right femur in dorsal (H) and ventral (view). *Abbreviations*: af, anterior facet; aif, facet for the axial intercentrum; an, anterior notch; bpe, broken posterior end; bpe, bulbous posterior end; ccf, facet for the cervical centrum; dp, dorsal process; dpc, deltopectoral crest; ff, fibular facet; gf, glenoid facet; if, intercoracoid facet; pm?, predation marks; pn, posterior notch; rf, radial facet; sf, scapular facet; tf, tibial facet; uf, ulnar facet; vp, ventral process. Scale bars represent 3 cm.

Figure 8. Surface models (generated from CT scan data) of the reassembled skull of BMT 1955.G35.1, *Protoichthyosaurus prostaxalis,* highlighting differences between fossil bone (grey), regions reconstructed during original reassembly in the 1950s (yellow), and regions

reconstructed in the course of the current work (blue). Right (A) and left (B) lateral, and dorsal (C) and ventral (D) views of the upper and lower jaws.

Figure 9. Surface models (generated from CT scan data) of the skull of BMT 1955.G35.1, *Protoichthyosaurus prostaxalis,* after the removal of minor damage and duplication/mirroring of asymmetrically preserved elements, and digital articulation of individual bones to produce a more accurate digital 3D reconstruction. Displacement of the lower jaw and premaxillae and nasals are the result of deformation (see text). Left lateral (A), dorsal (B), ventral (C), anterior (D), and posterior (E) views of the upper and lower jaws. Individual bones labeled using the same colors as Figures 2–4.

Figure 1

Three-dimensional skull of BMT 1955.G35.1, *Protoichthyosaurus prostaxalis*.

A, original photograph of the first skull reconstruction (left lateral view) within a couple of years of the 1955 excavation. Note that the prefrontal and postorbital are present, which we have been unable to locate in our study. B, skull in left lateral view, as reconstructed in 2015. C, skull in right lateral view, as reconstructed in 2015. Note the distinctive asymmetric maxilla with long, narrow anterior process. Teeth are not in their original positions. Scale bar represents 20 cm.

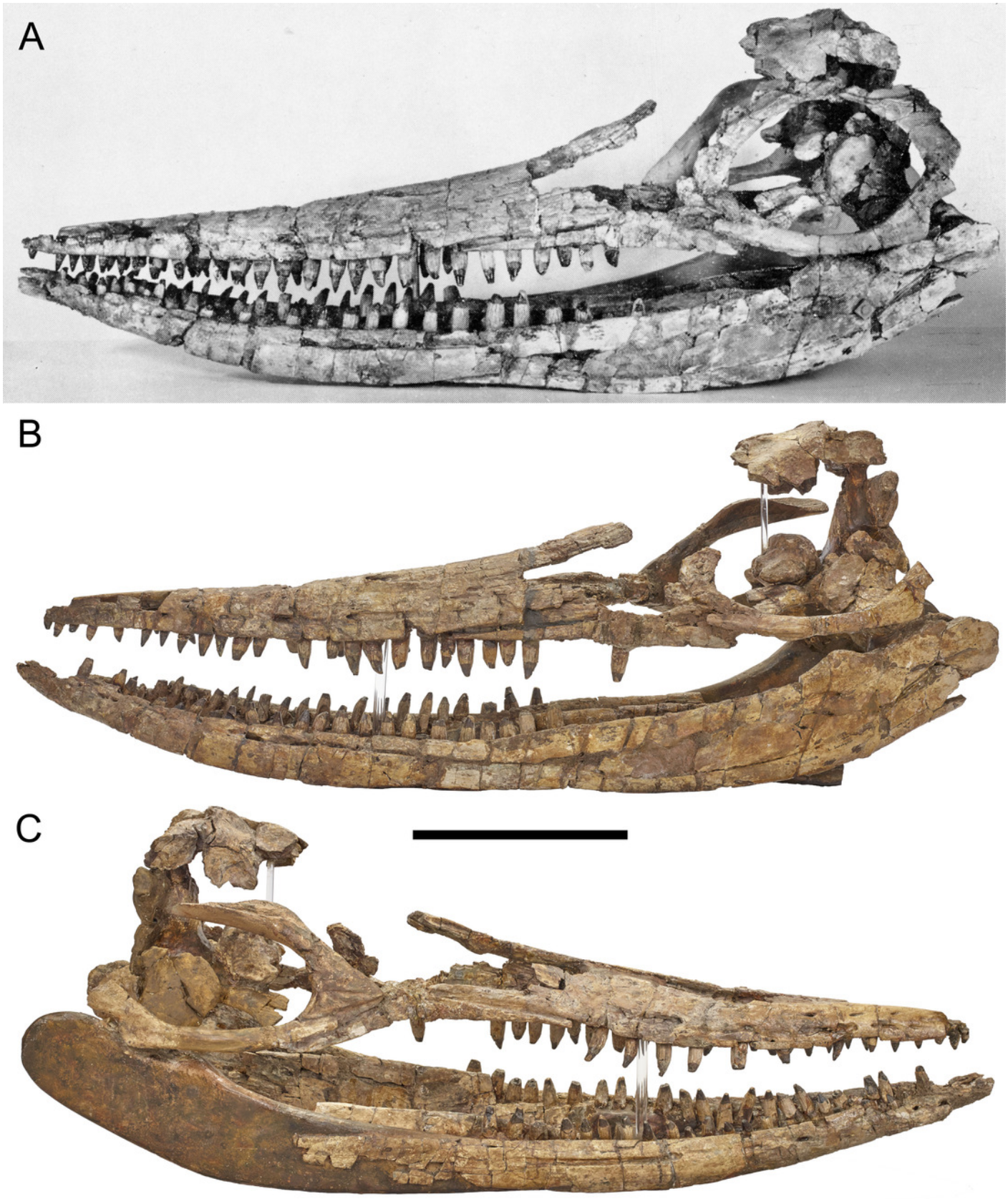
A
B
C

Figure 2

Surface models (generated from CT scan data) of preserved bones from the upper jaw of BMT 1955.G35.1, *Protoichthyosaurus prostaxalis*.

Right (A) and left (B) lateral views of the cranium. Medial views of the right (C) and left (D) sides of the cranium. Dorsal (E) and ventral (F) views of the cranium. Lateral views of the right (G) and left (H) premaxillae. Dorsal views of the right (I) and left (J) premaxillae. Posterior (K) view of the upper jaw. Individual bones are shown in different colours. Bones in G–J are transparent to visualize internal canals (shown in red opaque). Teeth are not in their original positions. *Abbreviations*: bs, basioccipital; ex, exoccipital; f?, possible fragment of frontal; j, jugal; l, lacrimal; mx, maxilla; n, nasal; p, parietal; pf, prefrontal; pmx, premaxilla; pt, pterygoid; q, quadrate; so, supraoccipital; sp, supratemporal; st, stapes. Scale bars equal 10 cm.

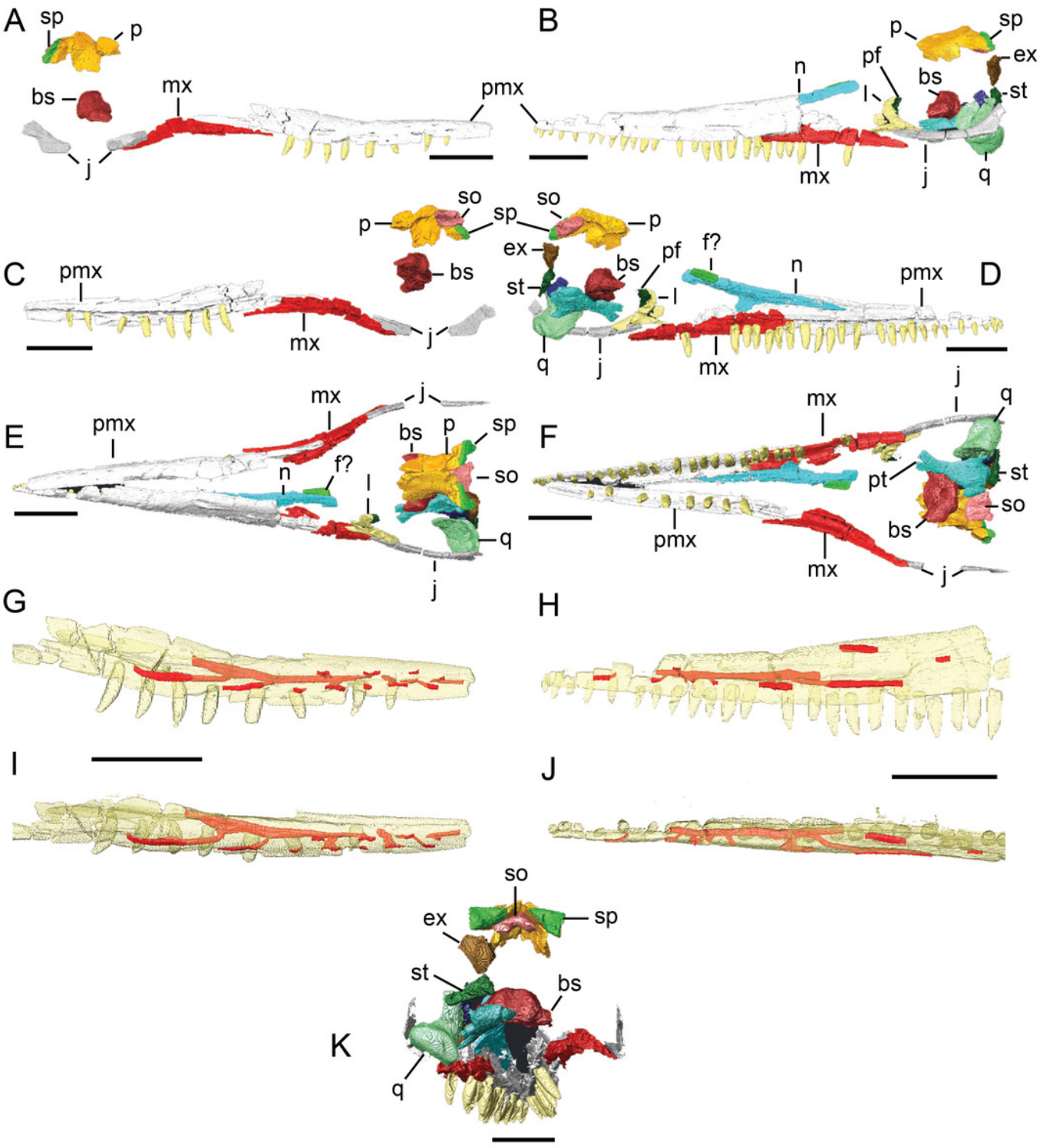
A
sp
p
bs
mx
pmx
j
B
p
sp
ex
pf
n
bs
st
l
mx
j
q
so
p
sp
so
p
ex
bs
pf
f?
st
n
pmx
C
pmx
bs
mx
j
D
q
j
mx
E
mx
j
pmx
bs
p
sp
n
f?
so
l
q
j
F
mx
j
q
pt
st
so
bs
pmx
mx
j
G
H
I
J
so
ex
sp
st
bs
K
q

Figure 3

Surface models (generated from micro-CT scan data) of preserved palatal and braincase bones from BMT 1955.G35.1, *Protoichthyosaurus prostaxalis*.

Right medial (A) and left lateral (B) views, dorsal (C) and ventral (D) views, and anterior (E) and posterior (F) views. Isolated supraoccipital in right anterolateral view (G). Individual bones are shown in different colours. Supraoccipital in G is transparent to visualize internal canals (shown in red opaque). *Abbreviations*: bs, basioccipital; ex, exoccipital; f?, probable fragment of upper pterygoid wing; p, parietal; pt, pterygoid; q, quadrate; se, sella turcica; so, supraoccipital; sp, supratemporal; st, stapes. Scale bars equal 10 cm, except for (G) which equals 5 cm.

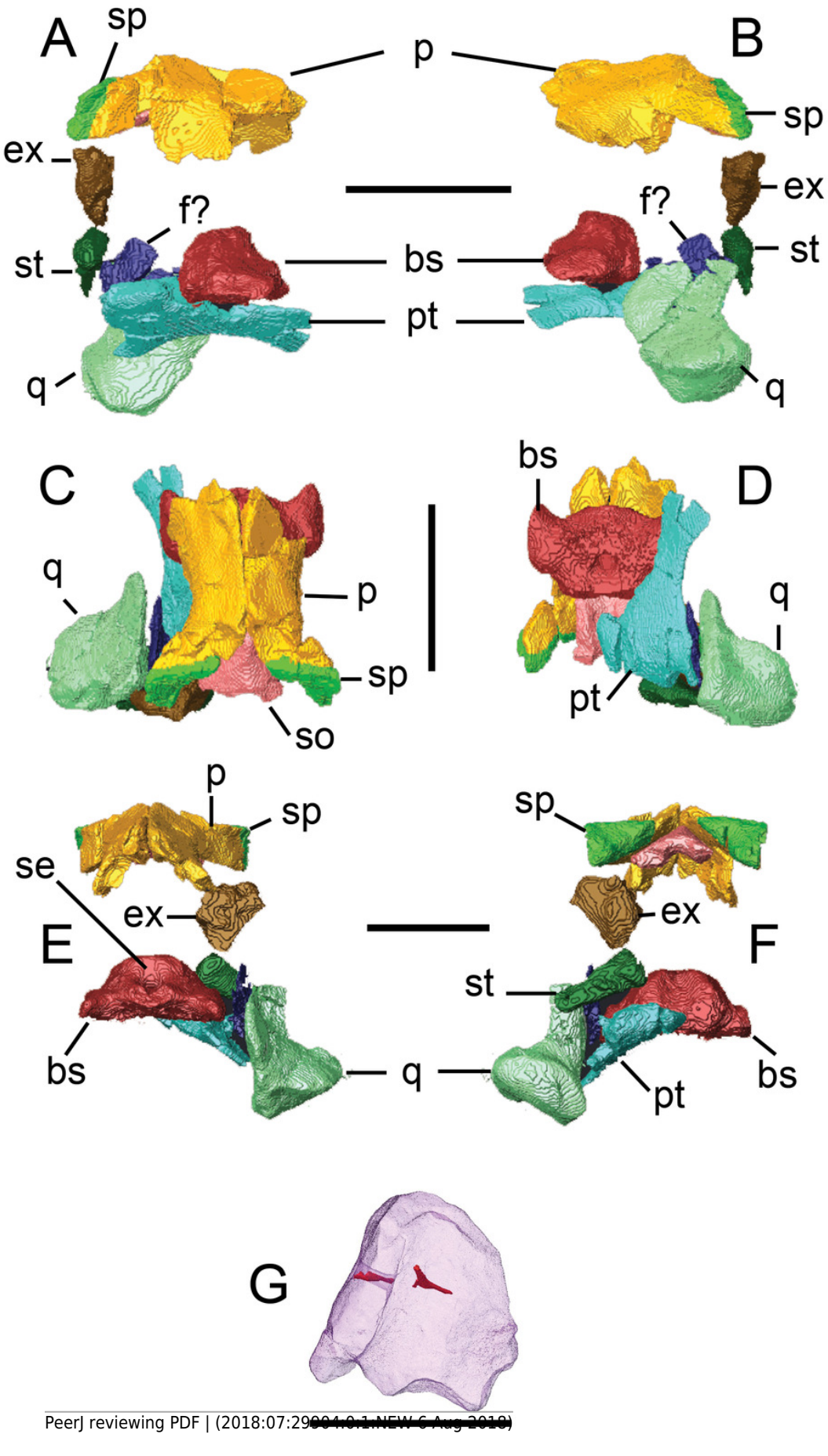
A
sp
p
B
sp
ex
ex
f?
f?
st
st
bs
pt
q
q
C
bs
D
q
p
q
sp
pt
so
p
sp
sp
se
ex
ex
E
F
st
bs
q
pt
bs
G

Figure 4

Surface models (generated from CT scan data) of preserved bones from the lower jaw of BMT 1955.G35.1, *Protoichthyosaurus prostaxalis*.

Lateral views of the right (A) and left (B) lower jaws. Medial views of the right (C) and left (D) lower jaws. Dorsal (E) and ventral (F) views of the both halves of the lower jaws. Lateral views of the right (G) and left (H) dentary. Ventral views of the right (I) and left (J) dentaries. Lateral oblique (K) view of the left surangular. Individual bones are shown in different colours. Bones in G–K are transparent to visualize internal canals (shown in red opaque). Teeth are not in their original positions. *Abbreviations*: an, angular; ar, articular, d, dentary; f?, possible surangular fragment; sa, surangular; sp, splenial; spf, splenial fragment. Scale bars equal 10 cm.

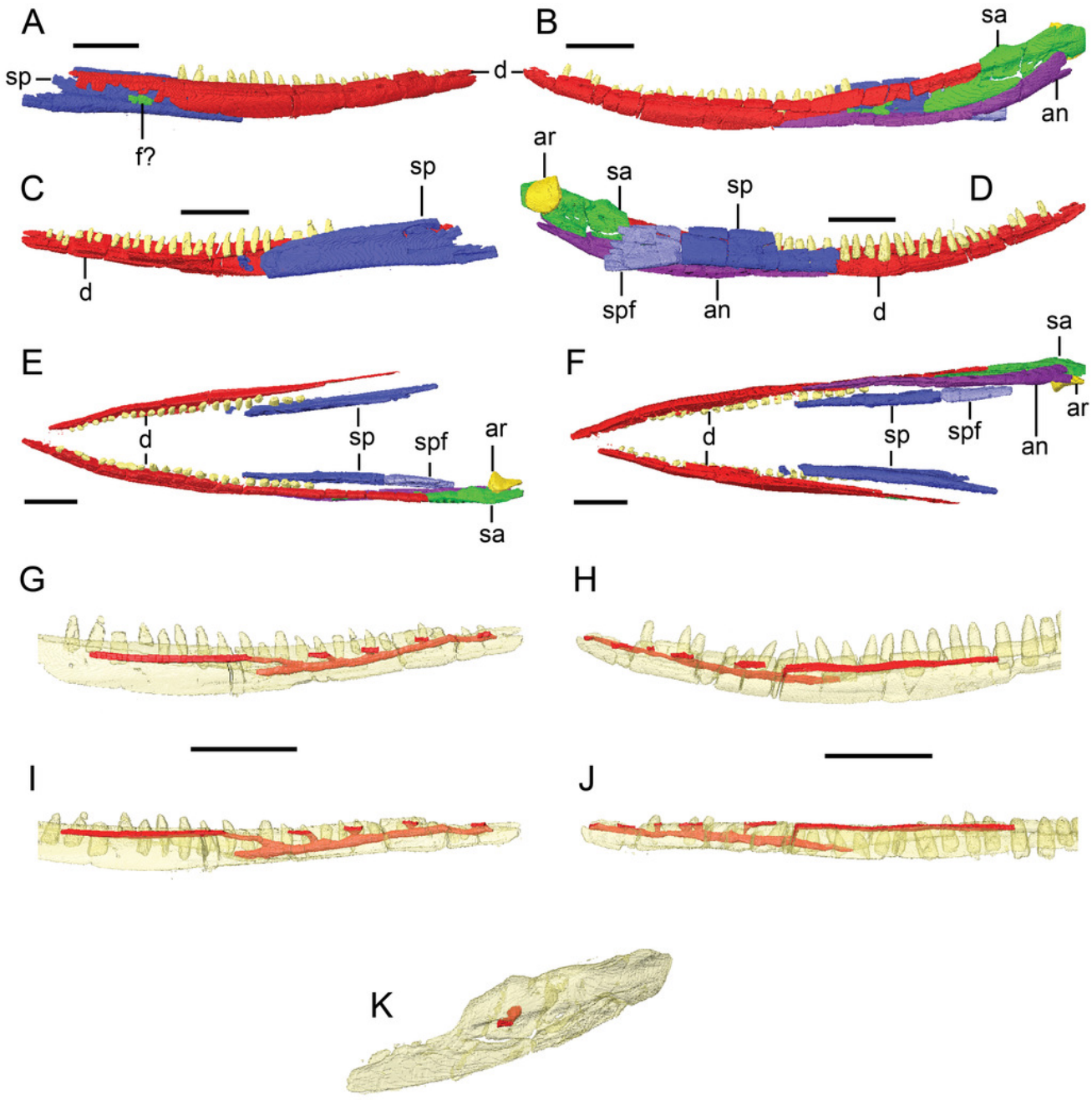
A
sp
f?
d
B
sa
an
C
sp
d
ar
sa
sp
D
spf
an
d
E
d
sp
spf
ar
sa
F
sa
ar
d
sp
spf
an
G
H
I
J
K

Figure 5

Elements of the skull, palate, lower jaw and dentition of BMT 1955.G35.1, *Protoichthyosaurus prostaxalis*.

A-D, incomplete and damaged, articulated parietals in dorsal (A), ventral (B), posterior (C) and anterior (D) view. E-F, incomplete and damaged left pterygoid in posterior (E) and ventral (F) view. Note the three wing-like projections in posterior view. G-I, incomplete and damaged left quadrate in anterior (G), posterior (H) and lateral (I) view. J, hyoids in dorsal view. K, practically complete tooth missing the tip of the crown. Note that the root is large with prominent grooves that extend to the base of the crown and continue as longitudinal striations on the crown. *Abbreviations*: ac, articular condyle; (?)ce, impression of cerebellum; ch, impression of cerebral hemisphere; dpf, descending parietal flange; eed, extra-encephalic depression; ocl, occipital lamella; ol, impression of optic lobe; op, elongate openings in the posterior surface of the parietal; par, palatal ramus; ps, parietal shelf (ridge); qf, quadratojugal facet; sc, sagittal crest; spt, supratemporal probably fused with parietals; vs, ventral surface. Scale bars represent 3 cm.

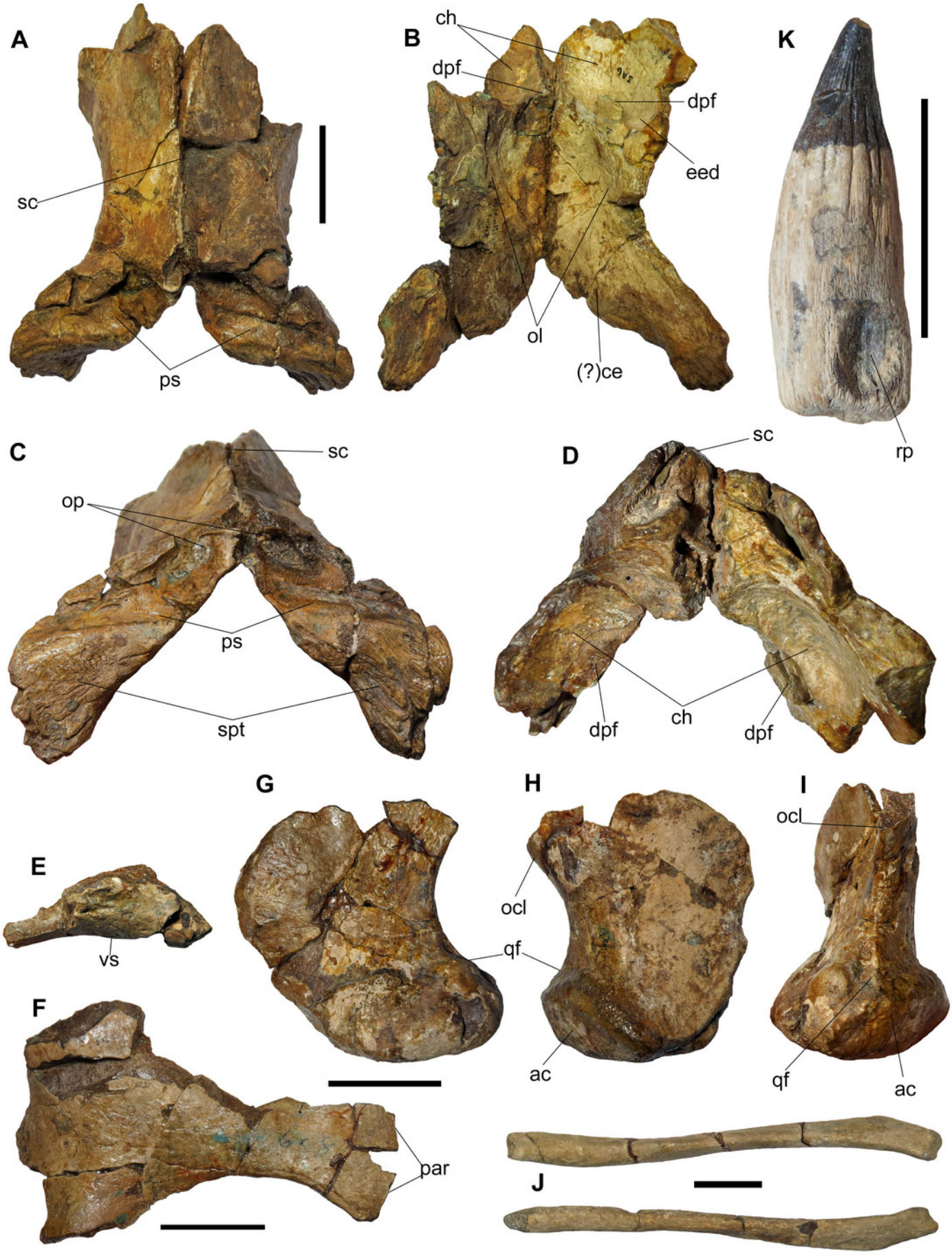
A
sc
ps
B
ch
dpf
dpf
eed
ol
(?)ce
K
rp
C
sc
op
ps
spt
D
sc
dpf
ch
dpf
E
vs
F
par
G
qf
H
ocl
qf
ac
I
ocl
qf
ac
J

Figure 6

Braincase elements of BMT 1955.G35.1, *Protoichthyosaurus prostaxalis*.

A-C, incomplete supraoccipital in posterior (A), dorsal (B) and ventral (C) view. D-E, parabasisphenoid with complete basisphenoid and broken parasphenoid in anterior (D) and ventral (E) view. F-G, left opisthotic in anteromedial (F) and ventrolateral (G) view. Note the 'V-shaped' membranous impression in F. H, incomplete left stapes in posterior view. *Abbreviations*: bf, facet for basipterygoid facet; bof, basioccipital facet; bp, basipterygoid process; cf, carotid foramen; ds, dorsum sellae; ef, exoccipital facet; hsc, horizontal semicircular canal; (?)ma, muscle attachment; mh, medial head; mr, median ridge; p, base of parasphenoid; pp, paroccipital process; pvsc, posterior vertical semicircular canal; rfm, roof of foramen magnum; sac, sacculus; sf, stapedial facet; st, sella turcica; t, paired trabeculae; tg, trenchant groove; (?)ut, utriculus. Scale bars represent 3 cm.

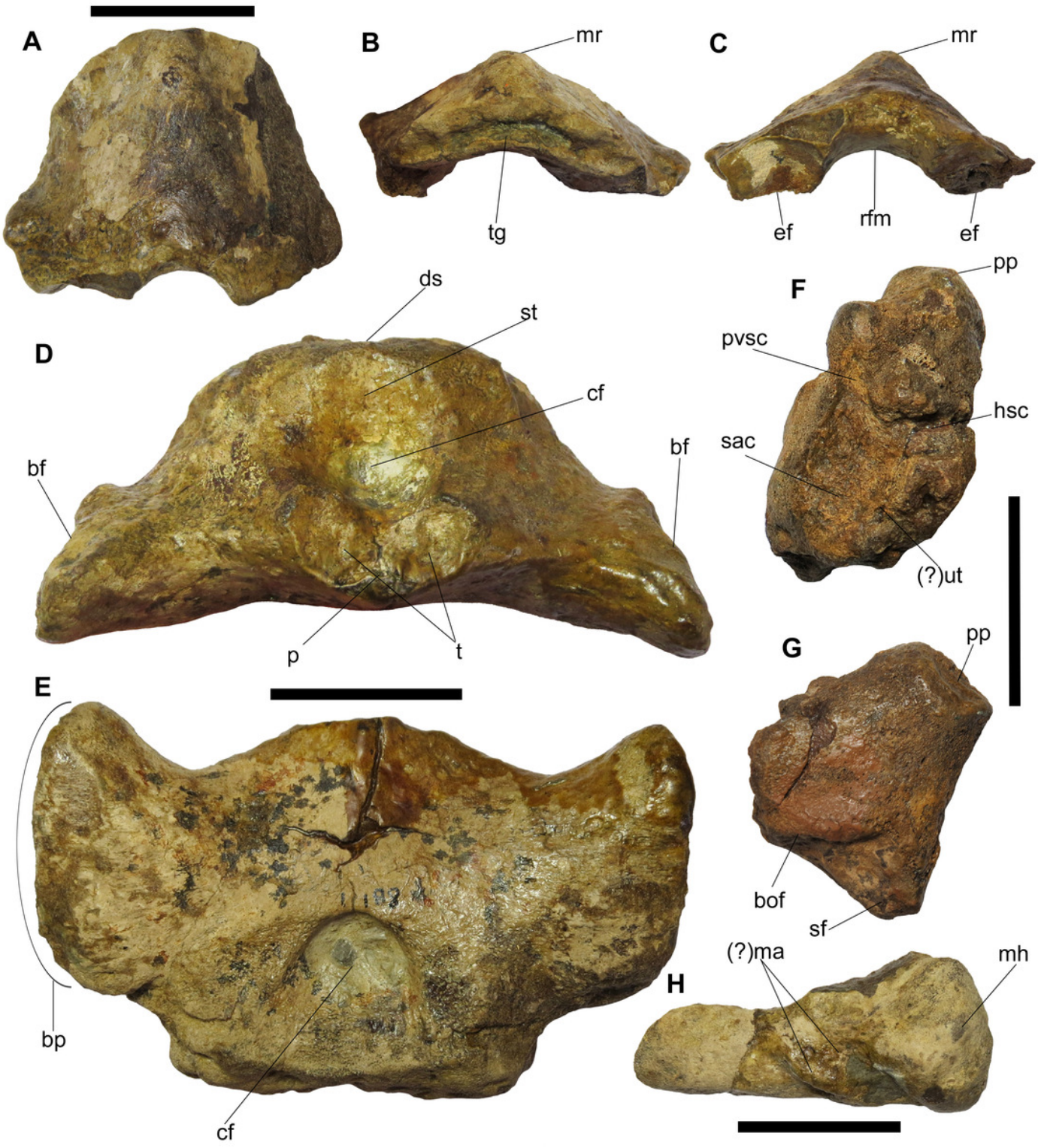
A
B
mr
tg
C
mr
ef
rfm
ef
D
ds
st
cf
bf
bf
p
t
E
bp
cf
F
pp
pvsc
hsc
sac
(?)ut
G
pp
bof
sf
H
(?)ma
mh

Figure 7

Elements of the postcranial skeleton of BMT 1955.G35.1, *Protoichthyosaurus prostaxalis*.

A-B, probable ‘unfused’ (see text for details) axis vertebra in anterior (A) and ventral (B) view. Note the unusual, almost rugose anterior surface rarely seen in ichthyosaurs. The dark, circular element to the right is a poorly preserved bivalve mollusc. C, left coracoid in dorsal view. D, incomplete left scapula in lateral view. E-F, left humerus in dorsal (E) and ventral (F) view. Note that the dorsal process (trochanter dorsalis) is damaged, as is the facet for the ulna. G, complete ilium in either lateral or medial view. Note that the posterior end (to the right) is bulbous, relative to the shaft. H-I, damaged (?)right femur in dorsal (H) and ventral (view). *Abbreviations*: af, anterior facet; aif, facet for the axial intercentrum; an, anterior notch; bpe, broken posterior end; bpe, bulbous posterior end; ccf, facet for the cervical centrum; dp, dorsal process; dpc, deltopectoral crest; ff, fibular facet; gf, glenoid facet; if, intercoracoid facet; pm?, predation marks; pn, posterior notch; rf, radial facet; sf, scapular facet; tf, tibial facet; uf, ulnar facet; vp, ventral process. Scale bars represent 3 cm.


A
B
aif
ccf
sf
an
C
gf
if
pn
E
dp
af
rf
uf
D
bpe
G
bpe
F
dpc
pm?
pm?
uf
rf
af
H
dp
ff
tf
I
vp
tf
ff

Figure 8

Surface models (generated from CT scan data) of the skull of BMT 1955.G35.1, *Protoichthyosaurus prostaxalis,* highlighting differences between the original skull and reconstruction.

Fossil bone (grey), regions reconstructed during original reassembly in the 1950s (yellow), and regions reconstructed in the course of the current work (blue). Right (A) and left (B) lateral, and dorsal (C) and ventral (D) views of the upper and lower jaws.

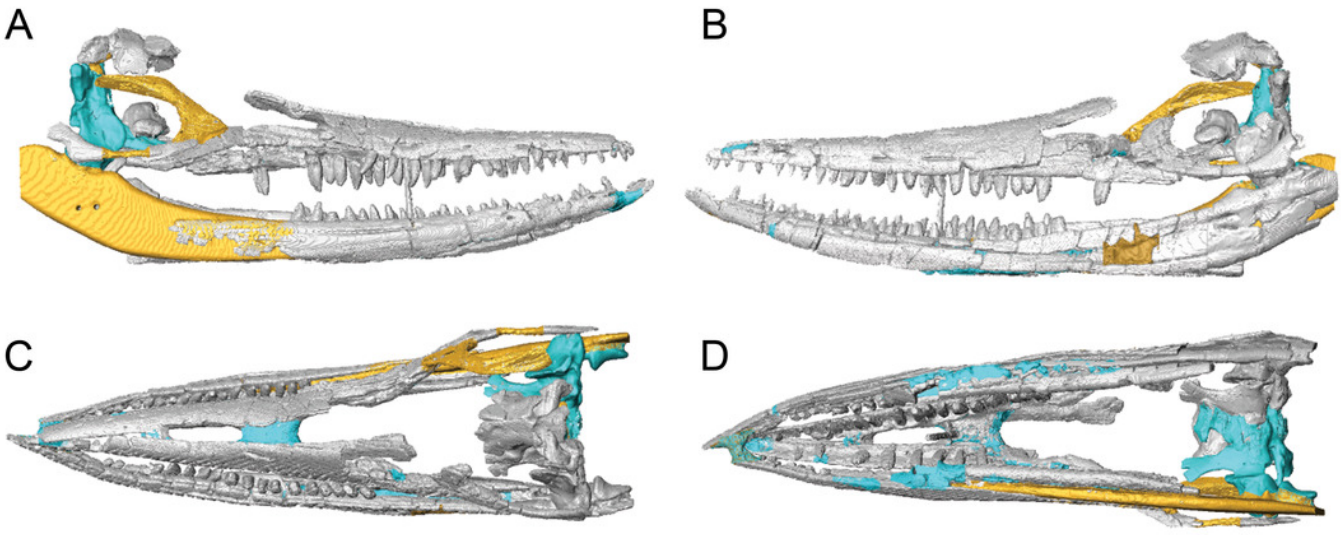

Figure 9

Surface models (generated from CT scan data) of the skull of BMT 1955.G35.1, *Protoichthyosaurus prostaxalis,* after removal of minor damage and duplication of asymmetrically preserved elements.

Surface models (generated from CT scan data) of the skull of BMT 1955.G35.1, *Protoichthyosaurus prostaxalis,* after the removal of minor damage and duplication/mirroring of asymmetrically preserved elements, and digital articulation of individual bones to produce a more accurate digital 3D reconstruction. Displacement of the lower jaw and premaxillae and nasals are the result of deformation (see text). Left lateral (A), dorsal (B), ventral (C), anterior (D), and posterior (E) views of the upper and lower jaws. Individual bones labeled using the same colors as Figures 2–4.

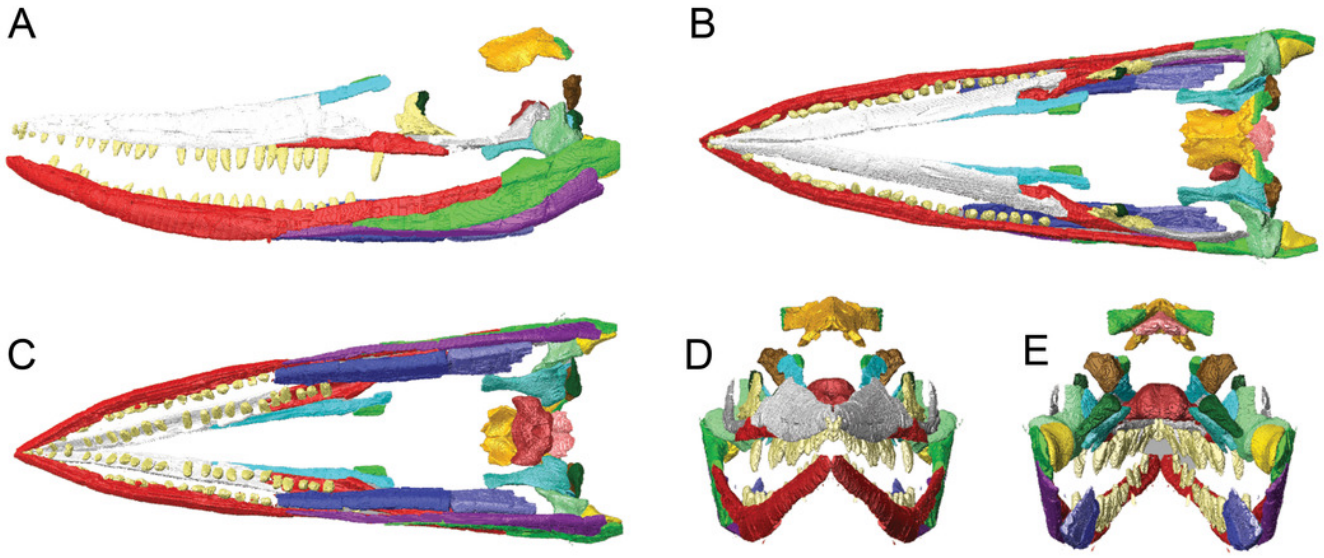

Table 1(on next page)

Measurements of some skull and postcranial elements of BMT 1955.G35.1, *Protoichthyosaurus prostaxalis*.

‘Width’ for fin elements refers to the anteroposterior dimension, perpendicular to the long axis of the fin. L and R denote measurement of left or right elements. Asterisk denotes an estimate because the bone is damaged or elements are missing.

Table 1

Measurements of some skull and postcranial elements of BMT 1955.G35.1, *Protoichthyosaurus prostaxalis*. 'Width' for fin elements refers to the anteroposterior dimension, perpendicular to the long axis of the fin. L and R denote measurement of left or right elements. Asterisk denotes an estimate because the bone is damaged or elements are missing.

Element	(cm)
Skull length	80*
Maxilla length	25.5R 24.2L*
Lower jaw length	87*
Basisphenoid length	5.82
Basisphenoid width	9.95
Supraoccipital height	5.04
Supraoccipital width	6.11
Quadrate length	9.4
Quadrate max width	8.2
Hyoid length	18.5R 18.2L
Coracoid med-lat length	12.16
Coracoid ant-post	13.66
Scapula preserved length	12.9*
Scapula proximal end only	7.25
Humerus length	10.4
Humerus distal width	8.59*
Humerus proximal width	7.66
Femur length	8.7
Femur distal width	5.1
Femur proximal width	2.5*
Ilium length	9.38
Humerus/Femur ratio	1.2